STRUCTURAL STUDIES OF A MEMBRANE EMBEDDED CHLORIDE CHANNEL FROM *E.COLI*, A PROKARYOTIC HOMOLOGUE OF CLC CHANNELS

Matthew William Bowler

Laboratory of Molecular Biophysics and New College,
Oxford University

A thesis submitted in partial fulfilment of the requirements for the degree of Master of Science *by research*

Trinity Term 2001

Structural Studies of a Membrane Embedded Chloride Channel from *E.coli,* a Prokaryotic Homologue of ClC Channels

Matthew William Bowler

Laboratory of Molecular Biophysics and New College, Oxford University

A thesis submitted in partial fulfilment of the requirements for the degree of Master of Science *by research*
Trinity Term 2001

Abstract

The ClC family of chloride channels are found throughout the eukaryotes and homologues are found among the prokaryotes. There are nine ClC chloride channels found in mammals that are expressed either ubiquitously or in specific tissues. They have a role in a broad spectrum of cellular functions, ranging from the control of electrical excitability of neurons and the maintenance of the balance of charge required in the acidification of organelles, to the regulation of cell volume. The physiological importance of these channels is often demonstrated by disease causing mutations. Mutations in ClC chloride channels cause myotonias, Becker's Disease and have been implicated in the spread of cancer.

The structural information on members of the ClC family is extremely limited. For this reason ClC prokaryotic homologues, ecClC1 and ecClC2 from *E.coli*, were cloned and expressed in the hope that this system would produce sufficient amounts of protein to grow crystals in order to obtain three-dimensional information. This information will provide a detailed mechanism of chloride conduction and molecular architecture of the channel necessary for the further physiological and pharmacological characterisation of this important family of chloride channels. The *E.coli* ClC chloride channel ecClC was cloned from *E.coli* genomic DNA and overexpressed in *E.coli*. The recombinant protein was purified from the *E.coli* membranes using detergents. Metal affinity and size exclusion chromatography were used to purify the protein to near homogeneity. Crystals of ecClC2 have been grown that diffract to 4Å and structural analysis is underway. This thesis describes the development of the purification protocol, the crystallisation of the protein and the preliminary analysis of the X-ray diffraction data.

Acknowledgements

I would first like to thank my supervisor, Dr. Declan Doyle. By introducing me to the field of membrane protein structural analysis, Declan gave the opportunity to dig myself out of a hole, something for which I shall always be grateful. I would also like to thank Professor Louise Johnson for her faith in me and for the opportunity to both work and study at the LMB. From G4, I would like to thank Thomas, Anling, Jenny and Jochen for help, advice and support. For friendship, advice, support and much more I thank (in no particular order) Jan, Simon, Nicole, Martin, Jane, Ed, Erica, Atlanta, John, Dave, Ian, Julie, Stefan, Maria, Elspeth, Rick, Sujit, Tom, Minakshi, Nick, Jasper, Jane Thorp, Richard, Annette and Catherine.

For proof reading and general support I thank my Father and Elspeth, two physicists who spent a huge amount of time on this thesis, I am very grateful for their efforts. I thank Mary for her constant support and timely advice, without which this thesis would not have been written.

This thesis is dedicated to those who made it possible, MGB, MJH and EFG and to the memory of PMB.

Matthew Bowler, 23rd August 2001

Contents

Chapter 3

Crystallisation of ecClC2 and X-ray Data Collection 44

Chapter 4

Further Work and Conclusion

Abbreviations

3C	Rhinovirus 3C protease
ATP	Adenosine triphosphate
Å	Angstrom
Bis/Tris	Bis(2hydroxyethyl)iminotris(hydroxymethyl)methane; 2-bis(2-hydroxyethyl)amino-2-(hydroxymethyl)-1,3-propanediol
bp	Base pairs
CAPS	3-(cyclohexylamino)-1-propanesulphonic acid
CBS	Cystathione-β synthase domain
CHES	2-N-(cyclohexylamino) ethanesulphonic acid
ClC	Member of the voltage dependent ClC family of chloride channel
CMC	Critical Micelle Concentration of a detergent
C-terminal	Carboxy terminal end of a protein
Da	Dalton
ddH_2O	Double distilled water
DM	*n*-Decyl-β-D-thiomaltoside
DME	Dimethyl ether
DNA	Deoxyribose nucleic acid
ecClC1	An *E.coli* ClC type channel
ecClC2	An *E.coli* ClC type channel, the product of *YadQ*
EDTA	Ethylenediaminetetraacetic acid
HEPES	N-(2-hydroxyethyl)piperazine-N'-(2-ethanesulphonic acid)
His_6	Hexa-Histidine tag
IPTG	Isopropyl- β-D-thiogalctopyranoside
LB	Luria-Bertani broth
LDAO	Lauryl diethylamine N-oxide
MAD	Multiple-wavelenghth anomalous dispersion
MCS	Multiple cloning site (of an expression plasmid)

MME	Monomethyl ether
N-terminal	Amino terminal end of a protein
OD_{xxx}	Optical density at XXXnm
PCR	Polymerase chain reaction
PEG	Polyethylene glycol
PMSF	Phenylmethylsulphonyl fluoride
rpm	Revolutions per minute
SB	Super broth
SDS	Sodium dodecylsulphate
SDS-PAGE	Sodium dodecylsulphate polyacrylamide gel electrophoresis
SEC	Size exclusion chromatography
TB	Terrific broth
TEMED	N,N,N',N'-tetramethylethylenediamine
TEV	Tobacco etch virus protease
Tris	Tris(hydroxymethyl)aminomethane
UV	Ultra-violet light
V	Volts
v/v	Percentage volume per volume
w/v	Percentage weight per volume

List of Figures

Chapter 1

Chapter 2

Chapter 3

Chapter 4

Appendix

List of Tables

Chapter 2

Chapter 3

Appendix

CHAPTER 1:

INTRODUCTION TO THE ClC CHLORIDE CHANNELS

Introduction

The transport of ions across membranes is one of the most important functions to occur in biological systems. Ions are not able to cross the hydrophobic membranes themselves as lipid bilayers have a very low permeability to ions and polar molecules due to their low dielectric constants (Mueller and Rudin 1963); therefore diffusion of ions is generally assisted by proteins. These proteins either facilitate the movement of ions across naturally occurring electrochemical gradients or pump ions against these gradients. Channel proteins form a hydrophilic pore that spans the membrane and allows the ions to pass through the hydrophobic environment. Ion transport proteins, on the other hand, usually bind an ion and actively transport it across the membrane; this usually requires energy in the form of adenosine triphosphate (ATP). The gradients across membranes are used in a large number of physiological processes, from maintaining cell size to transduction of nerve impulses and cell signalling (Alberts *et al.* 1989). The vast majority of research into ion channels has been on cation channels, namely those that transport sodium, potassium, calcium and protons. However, the important role played by chloride currents in the physiology of organisms has only been realised in the last ten years. Chloride is the most common ion in biological systems and a range of proteins, adapted to the transport of chloride ions, exists in almost all organisms. Six classes of chloride channel have so far been identified: The calcium activated chloride channels; the cystic fibrosis transmembrane conductance regulator (CFTR); the voltage dependent anion-selective channels (VDAC); the γ-aminobutiric acid gated chloride channel (GABA); the glycine receptor chloride channel and the ClC voltage gated chloride channels (Valverde 1999). There are nine ClC chloride channels found in mammals that are expressed either ubiquitously or in specific tissues (Jentsch and Gunther 1997). They have a role in a broad spectrum of cellular functions, ranging from the control of

electrical excitability of neurons and the maintenance of the balance of charge required in the acidification of organelles, to the regulation of cell volume (Waldegger and Jentsch 2000) (Maduke *et al.* 2000). ClC channels have also been found in many other organisms (Fig. 1.1) (Jentsch *et al.* 1999). The physiological roles of most of these channels remain unknown.

The ClC family of voltage gated chloride channels is structurally distinct, not only from ion channels in general but also from other chloride channels. The structural difference arises as the ClC channels are thought to be homodimers containing two distinct pores, as opposed to the usual pore architecture of oligomers of subunits forming a single central pore. As the pores are formed by two subunits, the residues that form the conductance channel are spread throughout the protein rather than potassium channels where the residues of the selectivity filter are contiguous (MacKinnon 1995). This feature has made identification of the pore forming residues very difficult. The ClC channels have between 10 and 12 transmembrane helices, as determined by hydropathy plots and mutational analyses, and both the N and C termini are cytoplasmic (Schmidt-Rose and Jentsch 1997). While there are many gaps in the knowledge of transmembrane topology a comparatively large amount is known about the electrophysiological properties of these channels.

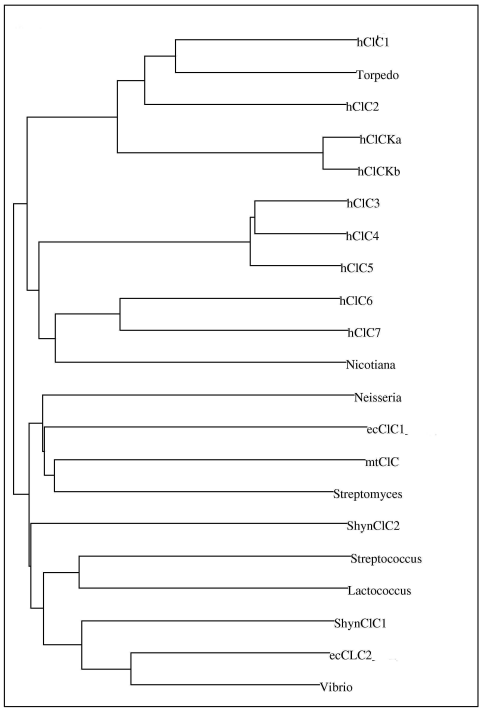

Fig 1.1. Phylogenetic tree showing the relationship between human, eukaryotic and prokaryotic ClC chloride channels. Torpedo: *Torpedo marmorata* ClC-0; hClC: human ClC channel; Nicotiana: *Nicotiana tobacum*; ecClC: *E.coli*; mtClC: *M.tuberculosis*; Shyn: *Synechocytis*; Vibrio: *Vibrio cholerae*; Lactococcus: *Lactococcus lactis*; Streptococcus: *Streptococcus thermophilus*; Streptomyces: *Streptomyces coelicolor*; Neisseria: *Neisseria meningitides.*
The tree was drawn using clustalW (Thompson *et al.* 1994).

Structure of the ClC channels

The first ClC chloride channel to be sequenced was ClC-0 from the electric organ of the ray *Torpedo marmorata* (Jentsch *et al.* 1990). The channel was originally thought to have 13 membrane spanning domains, this included a C-terminal domain now known to be cytosolic. Subsequent experiments have shown that there are between ten and twelve transmembrane helices, and sections of the channel have been demonstrated to be either extracellular or cytosolic by scanning mutagenesis techniques (Fig. 1.3) (Schmidt-Rose and Jentsch 1997). Figure 1.2 shows a hydropathy plot of ClC-0, the first seven transmembrane sections are plotted fairly unambiguously; however, the last section could indicate three or five helices. There is also another putative transmembrane domain at the C-terminal end of the protein; this has been found to be the second of two cystathionine-β synthase (CBS) domains (Bateman 1997) which are thought to be important as cellular location signals (Schwappach *et al.* 1998) and may play a part in channel gating (Beck *et al.* 1996) (Maduke *et al.* 1998).

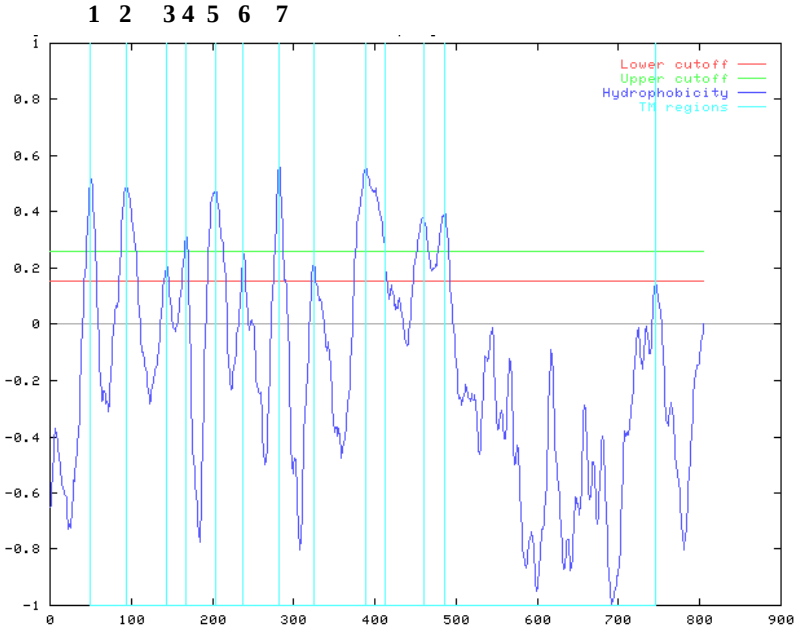

Fig. 1.2 Hydropathy plot of the sequence of ClC-0 from *Torpedo marmorata* using TOPPRED (Claros and von Heijne 1994) (http://bioweb.pasteur.fr/seqanal/interfaces/ toppred.html). Average hydrophobicity is shown by the blue trace and putative transmembrane segments are indicated by light blue bars and are numbered 1 to 7. The x axis shows the amino acid number, N to C-terminal.

1.2.1 ClC PORES

The ClC family of voltage gated chloride channels has a unique pore architecture consisting of a homodimer of subunits which form two independent pores (Middleton *et al.* 1996). Each pore is believed to be formed from a separate subunit or by the interface between them (Middleton *et al*. 1996). This architecture was first ascertained with ClC-0 (Hanke and Miller 1983) (Miller and White 1984) and ClC-1 (the human skeletal muscle equivalent) (Saviane *et al.* 1999), although whether it is the same for ClC-1, and other ClC channels is still in dispute (Fahlke *et al.* 1997b) (Fahlke *et al.* 1998). ClC-2 may also have the same architecture (Nobile *et al.* 2000). Patch clamp single channel conductance experiments demonstrate the existence of two pores that act independently of each other (Ludewig *et al.* 1996). The single channel recordings on ClC-0 clearly show three levels of chloride conductance: no current and two conducting levels one of which is twice that of the other. These results demonstrate three states of the channel: closed, one pore open and both pores open. A slow gate opens or closes the pores together and a fast gate can close the pores independently of each other. As more ClC channels are analysed, the model proposed for ClC-0 appears to be common to all ClC channels. It is now generally accepted that this architecture applies to the entire family (Middleton, Pheasant et al. 1996); it has also been shown that one of the *E.coli* ClC chloride channels has a similar structural design (Maduke *et al*. 1999).

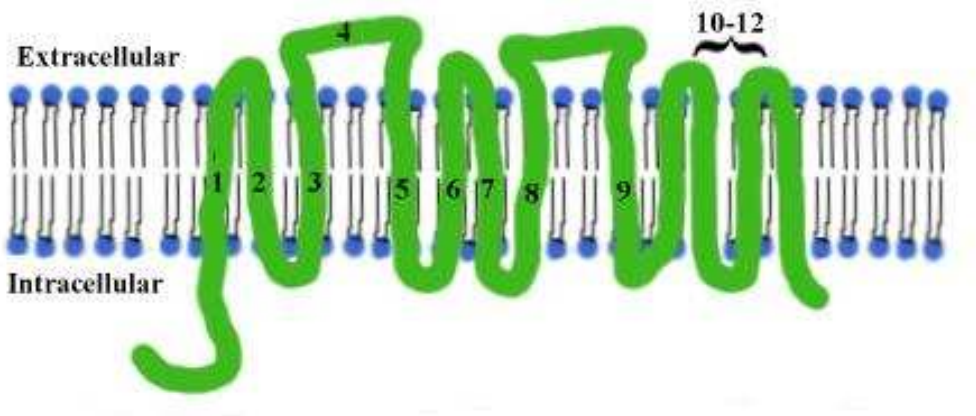

Fig. 1.3. Transmembrane topology model of the ClC channels according to Schmidt-Rose and Jentsch (Schmidt-Rose and Jentsch 1997). One monomer is displayed (green) within a lipid bilayer, the segment marked 10-12 is consists of either two or four helices and the location of the residues in the segment marked 4 is still in contention (Fahlke *et al.* 1997c).

1.2.2 ClC CHANNEL GATING

Although gating in the ClC channels is voltage dependent, there is no obvious voltage sensor in the primary structure, as there is in potassium and sodium channels (Papazian *et al.* 1991) (Stuhmer *et al.* 1989). In these channels the fourth transmembrane helix contains positively charged residues. These charged residues act as a voltage sensor and the protein is affected by changes in the transmembrane potential, causing a conformational change to open or close the pore (Sigworth 1994) (Larsson *et al.* 1996) (Yang *et al.* 1996). Several studies have shown that gating in ClC-0, both fast and slow, is not dependent on charged residues but on the extracellular chloride, or other anion, concentration (Pusch *et al.* 1995a) (Chen and Miller 1996) (Fahlke *et al.* 1997a). ClC-0 appears to be a chloride activated chloride channel, in that in the presence of chloride, channels are more likely to be open than those in the absence of chloride (Pusch 1996). The results of experiments performed so far have shown that the voltage dependency of the channel could be conferred on the channel by one of two possible mechanisms. The first suggestion is that voltage dependency occurs with the movement of chloride ions along 'binding' sites through the electric field (Pusch *et al.* 1995a). The second suggestion is that the movement of a bound chloride ion through the electric field during a conformational change imparts voltage dependency (Chen and Miller 1996). This mechanism of gating has also been demonstrated in ClC-1 and ClC-2 (Fahlke *et al.* 1997a) (Saviane *et al.* 1999) and in prestin, the outer hair cell motor protein, a chloride channel involved in cochlear amplification (Oliver *et al.* 2001). The C-terminal domain of both ClC-0 and ClC-1 is known to be involved in channel gating. Myotonic goats contain a mutation in the ClC-1 channel in the C-terminus that changes the voltage dependency of gating (Beck *et al*. 1996). Experiments have been conducted that express the transmembrane N-terminal domain of ClC-0 separately from the cytoplasmic C-terminal domain (Maduke *et al.* 1998). *Xenopus* oocytes expressing the transmembrane domain alone showed no measurable chloride current. The function of this domain was restored when co-expressed with the cytoplasmic C-terminal domain. These experiments demonstrate the importance of the C-terminal domain in channel function and gating. For the other ClC channels, gating is yet to be investigated. Gating that is independent of the pores has been demonstrated in some members of the ClC family;

this depends on their physiological role. For example, ClC-2, which is implicated in cell swelling, has been shown to have osmosensitive gating as well as voltage dependency (Grunder *et al.* 1992). There are also other gating mechanisms, such as response to pH (Stroffekova *et al.* 1998) (Bettendorff *et al.* 1995) and to hyperpolarisation (Jordt and Jentsch 1997) (Thiemann *et al.* 1992).

1.3 Physiological Functions of the ClC Family

The importance of some chloride channels was first discovered by the identification of diseases that are caused by malfunctioning channels. As the functions of more ClC channels are understood, a picture of their physiological importance is growing. This section describes the roles played by each of the ClC channels; the channels are grouped by their location and function, where appropriate.

1.3.1 ClC-1

Perhaps the best understood of the human chloride channels is ClC-1. It has the highest homology to the *Torpedo* channel ClC-0 (Fig. 1.1) and was the second ClC channel to be cloned (Steinmeyer *et al.* 1991b). This channel is expressed only in skeletal muscle (Steinmeyer *et al.* 1991a) and is responsible for the repolarisation of muscle action potentials. The high level of chloride conductance by ClC-1 in skeletal muscle is essential to the electrical stability of the membrane. Mutations in this channel are responsible for a variety of myotonias (Jentsch *et al.* 1995). These diseases are characterised by the inability of a muscle to relax after contraction, and the symptoms are of varying severity. These symptoms are caused by an inability to repolarise the membrane and return to the resting potential. The resting potential of axons is mediated by an efflux of potassium ions after the action potential is initiated by a massive influx of sodium ions (Alberts *et al.* 1989). In skeletal muscle, the resting potential is maintained by an inward chloride conductance (Steinmeyer *et al.* 1991b). A lowering or loss of the chloride current means the action potential of a stimulus cannot be repolarised and sodium channels are reactivated while the membrane is still depolarised. As the membrane is depolarised the sodium channels open, triggering another action potential along the nerve. This leads to many action

potentials along a nerve in response to a single stimulus (Koch *et al.* 1992). This phenomenon is referred to as the 'myotonic runs' and leads to the symptoms of myotonia. There are approximately forty-five separate point mutations that cause either dominant (Thomsen's disease) or recessive (Becker's disease) myotonia. These mutations are scattered across the protein. Thomsen myotonias are caused by mutations which result in a decrease in the sensitivity of the channel to transmembrane voltage. The channel can only be activated by abnormally high positive potentials that repolarisation of the action potential becomes impossible (Pusch *et al.* 1995b). Becker myotonias, however, are due to mutations that cause complete malfunction of the channel or reduce the conductance of the channel (Wollnik *et al.* 1997) which also lead to an inability to repolarise the membrane quickly. None of the myotonias are fatal due to the fact that even a mutation that leads to a malfunctioning protein only leads to a 50% reduction in chloride current. It is assumed that 100% reduction would be terminal. Some myotonias are due to malfunctioning sodium channels; however, the myotonias caused by ClC channels demonstrate the importance of ClC-1 in maintaining the plasma membrane potential in skeletal muscle.

1.3.2 ClC-2 AND ClC-3

ClC-2 is a chloride channel that is expressed throughout all tissues and is thought to be involved in cell volume regulation (Thiemann *et al.* 1992) (Jordt and Jentsch 1997) (Xiong *et al.* 1999). It has also been suggested that ClC-2 controls the concentration of chloride in neurons (Smith *et al.* 1995). ClC-3, again, is widely expressed but particularly in the brain and in skeletal muscle and has also been implicated in cell volume regulation (Duan *et al.* 1997) although a recent study points to a role in maintaining the pH of synaptic vesicles (Stobrawa *et al.* 2001). To date neither of these channels have been implicated in hereditary diseases due to mutations; however, both present themselves as interesting drug targets. ClC-2 has been found in the apical membranes of lung epithelia (Murray *et al.* 1995). This is the same tissue in which the cystic fibrosis transmembrane conductance regulator (CFTR) is expressed (Jovov *et al.* 1995). As ClC-2 remains closed most of the time (Grunder *et al.* 1992) it may be possible to make this protein replace the loss of

chloride conduction, caused in this tissue, by the malfunctioning CFTR (Jentsch *et al*. 1999). Perhaps a more promising area of therapy has emerged from the discovery of voltage dependent chloride currents, similar to those of ClC-2 and ClC-3, in malignant glioma cells of the brain (Ullrich *et al.* 1995) (Ullrich *et al.* 1996). The presence of ClC-2 has also been implied in rat astrocytes, found near brain blood vessels (Nobile *et al*. 2000). It is suggested that in the tumor cells the expression of the chloride channels is upregulated, allowing the cells to change their volume to a greater extent (Soroceanu *et al.* 1999). This may facilitate the movement of the cells through intercellular spaces and contribute to the spreading of the cancer. It has been demonstrated that ClC channel blockers, such as chlorotoxin from the venom of the scorpion *Leiurus quinquestriatus* and tamoxifen, prevent malignant glial cell migration *in vitro* (Ullrich *et al.* 1998) (Soroceanu *et al*. 1999) by reducing osmotically induced volume change. Other studies have found chloride currents expressed in cervical cancer cells that are absent in normal tissue (Chou *et al.* 1995) (Shen *et al.* 1996). While many factors contribute to the shrinking of cells and the proliferation of cancer, the discovery of a unique chloride current expressed in some cancers presents a very hopeful drug target to prevent or at least limit the spread of cancer. Further work has to be done to characterise the channels involved; however, specific inhibitors are already known and this work is at an exciting stage.

ClC-3 has recently been found in endosomes and synaptic vesicles where it probably plays a role similar to that of ClC-5 in dissipating the electrostatic charge generated by acidification of the vesicles (Stobrawa *et al*. 2001). Acidification of vesicles is necessary for a number of reasons, low pH is sometimes required for the activity of enzymes in the vesicles and is essential to endocytosis. A low pH is needed in synaptic vesicles as the proton gradient enables neurotransmitter uptake. Balancing the charge built up by the H^+ ATPase is essential to maintain efficient proton build up (Waldegger and Jentsch 2000).

1.3.3 ClC-Ka, ClC-Kb AND ClC-5

During the process of filtration that occurs in the glomerulus of the mammalian kidney, toxins in the blood are removed along with many other essential substances such as water, salts and small peptides. These molecules need to be

recovered from the nephron and this is achieved by moving ions back into the blood. Chloride channels are an essential part of this process to maintain hypertonicity in the kidney to reabsorb water and other processes. Their importance in the kidney is clear from diseases caused by channel malfunction, and mouse models, with kidney ClC channels knocked out. ClC-Ka and ClC-Kb are expressed exclusively in the kidneys (Adachi *et al.* 1994), ClC-5 is also expressed primarily in the kidneys (Gunther *et al.* 1998) but also in liver and brain tissue (Jentsch, Friedrich et al. 1999). The roles of these channels are better understood, again because of diseases associated with their malfunction. ClC-Ka and ClC-Kb are very homologous proteins that are about 90% identical; however, their distribution within the kidney is different and defects in them lead to different diseases.

Mutations in ClC-Kb lead to Type III Bartter's syndrome (Simon *et al.* 1997). This disease is characterised by salt loss in the thick ascending limb of Henle's loop (see fig. 1.4), as ions cannot be reabsorbed. This leads to very low concentrations of potassium and protons in the blood (hypokalaemia and alkalosis respectively) and an increase in the concentration of calcium in the urine (hypercalciuria). As the mutations in ClC-Kb reduce the ability of the channel to conduct chloride this leads to a build up of intracellular chloride ions in the renal tubules. The increase in chloride subsequently inhibits the NaK2Cl cotransporter as it cannot operate against the gradient; this leads to a build up of these ions in the urine (Fig. 1.4).

ClC-Ka is also involved in urinary concentration but disruption of this protein leads to very different symptoms to those of Bartter's syndrome. There are no mutations known to occur in ClC-Ka, but a knockout mouse model showed symptoms of diabetes insipidus (Matsumura *et al.* 1999). In this mouse model the gene for ClC-K1 was knocked out; this is assumed to be equivalent to hClC-Ka although the evidence is not conclusive. ClC-K1 localises in the thin ascending loop of Henle where chloride ions are transported into the medulla maintaining high salt concentrations required for water reabsorption. Malfunction in this protein will lead to the high water loss associated with diabetes insipidus.

Mutations in the ClC-5 gene lead to Dent's disease; this is characterised by hypercalciuria, the formation of kidney stones and low molecular weight proteinurea. Low molecular weight proteins are lost in the filtration that occurs in the Bowman's capsule; however, they are recovered in the proximal tubule by endocytosis. Once in

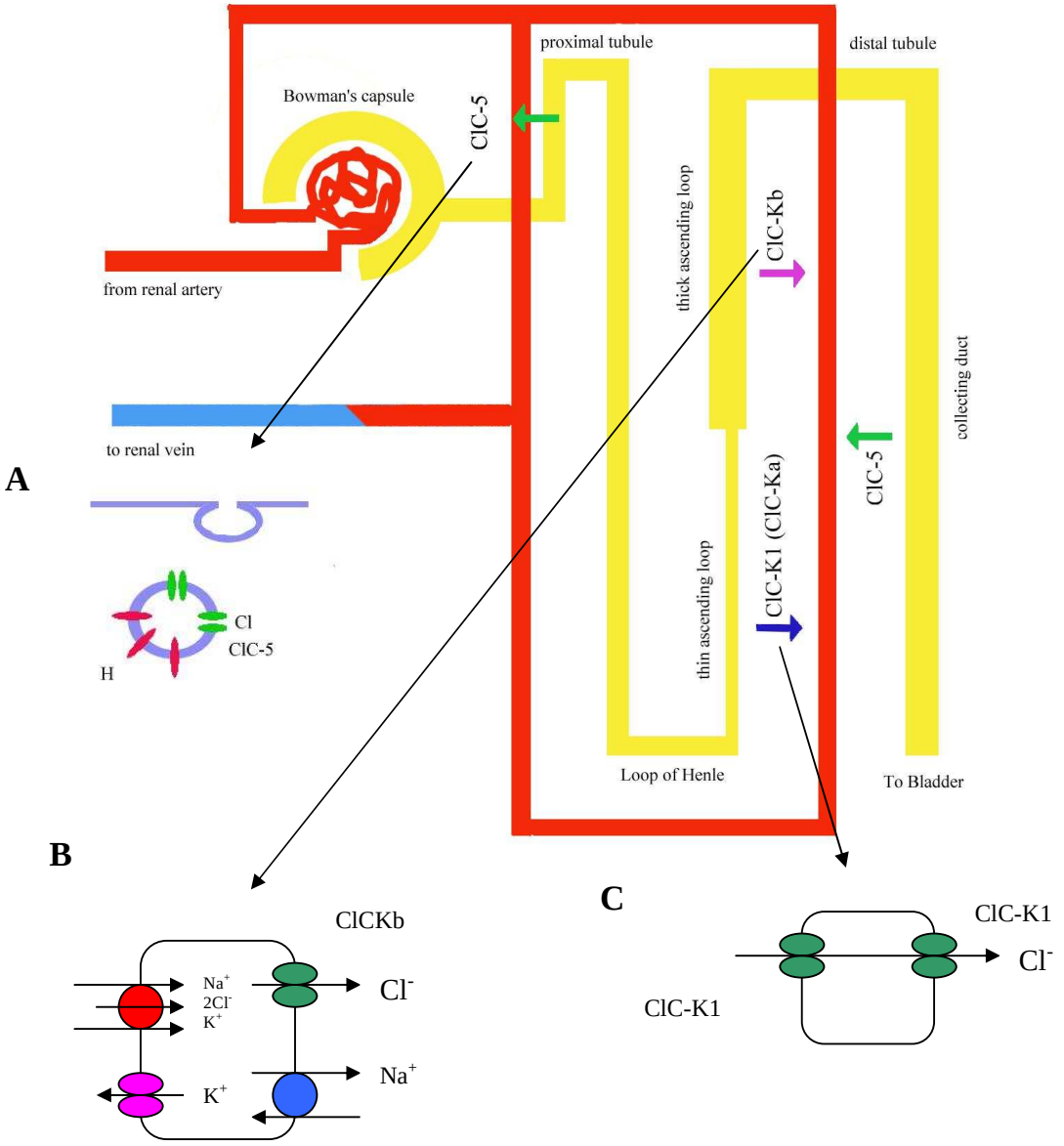

Fig. 1.4. Schematic of the human nephron and the role played by chloride channels in reabsorption. Capillaries surrounding the loop of Henle and the tubules are shown as red. **A:** Low molecular weight peptides lost in ultrafiltration are recovered in the proximal tubule by endocytosis, low pH is necessary for this process, ClC-5 (green) neutralises the high positive charge generated by the H^+ ATPase (red) in the endosome (blue). **B:** Salts are reabsorbed from the thick ascending loop by the NaK2Cl cotransporter (red), Chloride is then shunted out by ClC-Kb (green). Other forms of Bartter's syndrome are caused by mutations in NaK2Cl (red) and the ROMK potassium channel (purple). The cotransporter cannot operate if the gradient is not maintained; this leads to salt loss in the urine. **C:** Chloride is reabsorbed from the thin ascending loop by ClC-K1 (green); this maintains the hypertonicity of the surrounding fluids needed for water reabsorption. ClC-5 is also located in the collecting duct, however its exact role here remains unknown.

the cell these peptides are degraded in lysosomes. The endosomes formed in the uptake of peptides need to maintain a low pH. This is maintained by the H^+ ATPase. ClC-5 is coexpressed, in the proximal tubule, with the H^+ ATPase (Gunther *et al.* 1998), where it is thought that it performs the role of dissipating the electropotential across the membrane that is built up by the transport of protons into the endosome (Piwon *et al.* 2000). The more serious symptoms of Dent's disease, hypercalciuria which causes kidney stones and can lead to renal failure, are less easily explained. A mouse model with partial ClC-5 function demonstrated slightly increased levels of calcium in the urine but not to the levels observed in Dent's disease (Luyckx *et al.* 1999).

The number of diseases associated with chloride channel function in the kidney demonstrate their essential role in recovering solutes after ultrafiltration.

1.3.4 ClC-4 AND ClC-6

Both of these channels are widely expressed in all tissues and the roles are largely unknown. ClC-4 is similar to ClC-5 both in sequence and in physiological response; they show the same conductance and a similar response to pH. This implies a similar role for ClC-4 in the dissipation of positive charge produced during the acidification of vesicles by H^+ ATPase (Friedrich *et al.* 1999). ClC-6 has been found to in the endoplasmic reticulum with the Ca^+ ATPase (Buyse *et al.* 1998). The most likely role here is to neutralise the electrostatic charge generated by the accumulation of calcium ions.

1.3.5 ClC-7

The vital role that this member of the ClC family plays has only recently been elucidated. Similarly to ClC-3, 4, 5 and 6, ClC-7 mediates the chloride conductance to dissipate charge built up by ATPases (Brandt and Jentsch. 1995). ClC-7 is found in all tissues and yet its absence leads to osteopetrosis (Kornak *et al.* 2001). Osteopetrosis is a genetic disorder where bone is not reabsorbed, the opposite of osteoporosis. Bone reabsorption is needed to maintain blood calcium levels, bone

growth and healing and bone re-modelling (Vaananen *et al.* 2000). The bone is reabsorbed by osteoclasts, these are specialised cells that bind to bone and produce acidic vesicles containing proteases. These vesicles fuse with the outer membrane at the ruffled border (the space between cell and bone) and the bone is dissolved by the proteases and the acid produced by H^+ ATPase and ClC-7. If ClC-7 is absent or malfunctioning, the H^+ ATPase cannot efficiently pump protons into the ruffled border, thereby preventing the reabsorption of bone. A recent study found that osteopetrosis is caused by two mutations in the gene encoding ClC-7 (Kornak *et al.* 2001). It was also shown that ClC-7 deficient mice show all the symptoms of osteopetrosis.

The role of ClC chloride channels is varied and very important. As the functions of more members of the family are discovered, the potential for a deeper understanding of some diseases becomes apparent. If combined with a better structural view of ClC channels, this potential is increased.

Prokaryotic ClC Channels

Hydropathy plots of the prokaryotic ClC channels show a similar arrangement to the eukaryotic channels; again there is no clear definition of the number of helices at the C-terminal end (Fig. 1.6). Although sequence alignments between these channels and eukaryotic ClC channels show around 25% identity, the transmembrane helices are highly conserved as well as sequences identified as being important for gating and pore formation (Fig. 1.5). The sequence from residue 164 to 171 (using ClC-0 numbering) GKXGPXXH in eukaryotic ClCs is important in pore formation (Fahlke *et al*. 1997c) (Fahlke *et al.* 2001) (Fahlke 2001); this sequence is also highly conserved in prokaryotes, most sharing the sequence GREGPTXQ with a few exceptions (ecClC1 and the first *Synechocystis* channel). Another section thought to be important in ion conduction lies before the third transmembrane helix. This sequence, GSGIP (residues 122 to 126) in eukaria and GXGIP over all species (Fig. 1.5) has been shown to affect anion selection in ClC-1 (Ludewig *et al*. 1996) (Fahlke 2001). There are also seven highly conserved regions that lie in areas that are

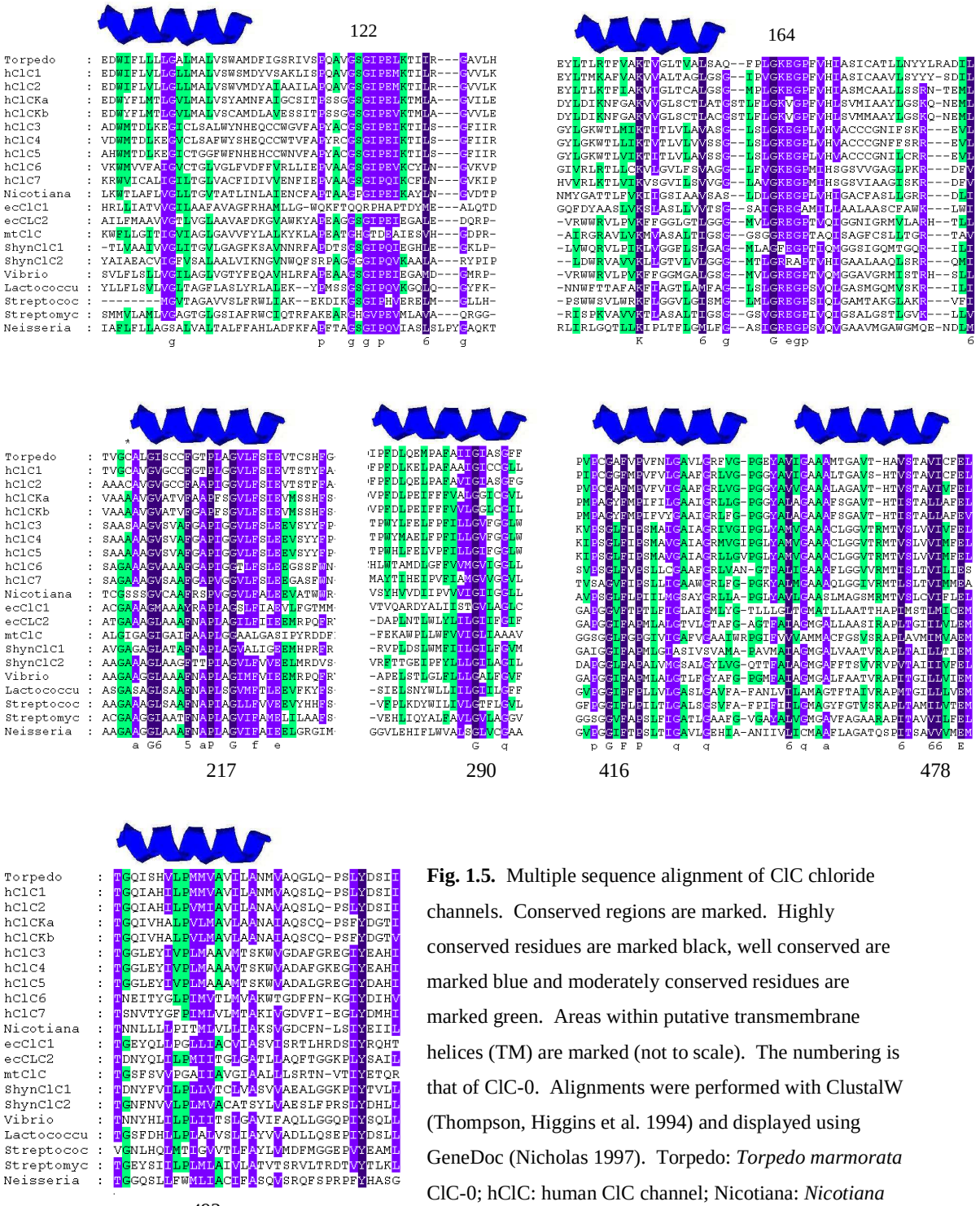

Fig. 1.5. Multiple sequence alignment of ClC chloride channels. Conserved regions are marked. Highly conserved residues are marked black, well conserved are marked blue and moderately conserved residues are marked green. Areas within putative transmembrane helices (TM) are marked (not to scale). The numbering is that of ClC-0. Alignments were performed with ClustalW (Thompson, Higgins et al. 1994) and displayed using GeneDoc (Nicholas 1997). Torpedo: *Torpedo marmorata* ClC-0; hClC: human ClC channel; Nicotiana: *Nicotiana tobacum*; ecClC: *E.coli*; mtClC: *M.tuberculosis*; Shyn: *Synechocytis*; Vibrio: *Vibrio cholerae*; Lactococcus: *Lactococcus lactis*; Streptococcus: *Streptococcus thermophilus*; Streptomyces: *Streptomyces coelicolor*; Neisseria: *Neisseria meningitides.*

probably transmembrane helices (Fig. 1.5). A proline (residue 217) that lies in the centre of transmembrane helix 5 (see figure 1.3), is conserved throughout all species. This residue has been implicated in the gating of the channel by causing a kink in the helix that can act as a hinge (Sansom and Weinstein 2000). This hinge may allow opening and closing of the channel (Tieleman *et al.* 2001). Many of the archea and bacteria, but not all, have ClC type chloride channels and most lack the CBS domain (with the exception of *A.fulgidus* and *Synechocystis*). Prokaryotes may use ClC channels in the dissipation of charge; however their function remains unknown.

The evidence from the primary structure of these prokaryotic proteins is that they are ClC type chloride channels (Fig. 1.6) and it has been shown that the *E.coli* chloride channel, when reconstituted into liposomes, is able to transport chloride ions and has a selectivity similar to that of eukaryotic ClC channels (Maduke *et al.* 1999) (Mindell *et al.* 2001).

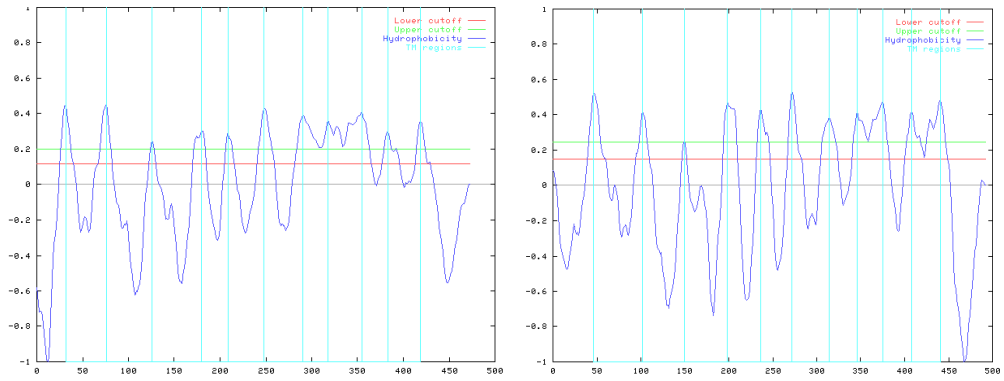

Fig. 1.6. Hydropathy plots of *E.coli* (left) and *M.tuberculosis* (right) ClC channels. The plots show 11 transmembrane helices rather than 12. The initial N-terminal sections show a similar plot to the *Torpedo* Channel (Fig. 1.2). Neither of these channels have a CBS domain.

A projection structure to 6.5Å of the product of *yadQ*, adds to the evidence that prokaryotic ClC channels have a similar structure to the eukaryotic ClC channels (Fig. 1.7) (Mindell *et al.* 2001). This structure, obtained from electron diffraction of two-dimensional crystals, does not answer any of the unresolved structural questions about the ClC family such as the number of transmembrane helices. However, it does show that the *E.coli* channel has homodimeric architecture and may have two pores,

although this cannot be determined conclusively from the data. This evidence demonstrates the likelihood that these prokaryotic proteins are faithful homologues of the eukaryotic ClCs.

Prokaryotic homologues of eukaryotic membrane proteins have been shown to be suitable targets for structural study (MacKinnon and Doyle 1997) (Doyle *et al.* 1998) (Fu *et al.* 2000) (Palczewski *et al.* 2000) as they can be readily over-expressed in simple systems. A great deal is known about the part played by ClC channels in human physiology and disease. However, without structural information the mechanism of anion selection, conduction and gating will be incomplete.

Figure 1.7 has been removed for copyright reasons.

Fig 1.7. Contour map of ecClC2 from electron diffraction of 2-dimensional crystals (Mindell *et al.* 2001). Two fold symmetry can be seen and perhaps 2 pores?

The aim of the present study was to obtain a high-resolution (<3 Å) three-dimensional structure of an *E.coli* chloride channel by X-ray crystallography. This thesis describes the cloning, high-level expression, purification and crystallisation of the *E.coli* ClC channel, ecClC2, the product of the *yadQ* gene. It also describes the analysis of preliminary X-ray diffraction data obtained with synchrotron radiation.

CHAPTER 2:

CLONING AND EXPRESSION OF *E.COLI* CHLORIDE CHANNELS

The basic requirement of structural studies by X-ray crystallography is the production and purification of the protein of interest in milligram quantities so that crystallisation trials can be undertaken. This is usually achieved by cloning the gene into a vector that will cause the host to overexpress the protein. This chapter describes the design and production of an expression system for the *E.coli* chloride channel, including the expression constructs that failed or were abandoned. Details of any procedures not explained in the following chapters can be found in the biochemical methods appendix.

2.1 Homology Search for *E.coli* ClC channels

Searches for proteins homologous to eukaryotic ClC chloride channels were performed with BLAST (Basic Local Alignment Search Tool) (Altschul *et al.* 1990) accessed at the National Centre for Biotechnology Information (NCBI) web site (www.ncbi.nlm.nih.gov/). The protein sequence of ClC-0 from *Torpedo marmorata* (Jentsch *et al.* 1990) was used as a ClC 'model' to compare with sequences in the database. The search of prokaryotic genomes (finished and unfinished) found thirty sequences similar to that of ClC-0, ranging from 21 to 25% sequence identity. Two ClC homologues were found in the *E.coli* genome. Both of the genes encoding ClC homologues, accession numbers AAC74664 (hereafter referred to as ecClC1) and C64739 (*yadQ*) (hereafter referred to as ecClC2), showed a sequence identity of 25%. These sequences code for hypothetical proteins of approximately 50kDa.

2.2 Purification of *E.coli* K-12 genomic DNA

Escherichia coli K-12 was purchased from ATCC (American Type Culture Collection, Manassas, VA, USA) as a lyophilised pellet. The pellet was resuspended in 1ml LB broth. 100ml of LB broth was then inoculated with 800µl of the resuspended pellet and grown at 30°C overnight in an orbital incubator at 200rpm. The cells were harvested by centrifugation at 5000rpm for 5 minutes in an Eppendorf centrifuge 5804R. Genomic DNA was purified using the High Pure PCR Template Preparation Kit (Roche Diagnostics, Ltd). The presence and purity of the genomic DNA was assessed by running samples on a 1% agarose gel (Fig. 2.1). Purified DNA was stored in 200µl aliquots at -80°C.

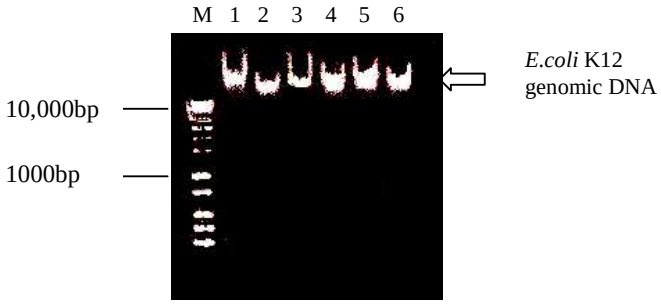

Figure 2.1 *E.coli* K-12 genomic DNA run on a 1% agarose gel stained in ethidium bromide for 30 minutes, visualised with UV light. The *E.coli* genome is 4.7 x 10^6bp in size and therefore barely leaves the wells in the gel. Lane M – Molecular weight markers (for a detailed diagram of molecular weight markers used in this project see biological methods appendix); lanes 1 to 6, aliquots 1 to 6 of *E.coli* K-12 genomic DNA.

2.3. Design of primers for PCR

The DNA sequences of the chloride channel encoding genes were obtained from NCBI. From these sequences synthetic primers, that corresponded to the 5' and 3' beginning and ends of the sequences, were designed. The design incorporated specific sequences recognised by a particular restriction endonuclease to enable the PCR product to be subsequently ligated into an appropriate vector (Fig.2.2).

Using the polymerase chain reaction (PCR) method the copies of the ClC genes in *E.coli* genome were amplified many times providing enough copies to clone the gene into a plasmid vector (Figs. 2.3 and 2.4). The sequences of the ClC genes were run through the programme tacg2 (www.cmbi.kun.nl/bioinf/tools/tacg/

tacg2.form.html). This programme predicts which restriction endonucleases will digest within the sequence and which will not, providing a list of enzymes that can be used to ligate the gene into a vector without digesting the gene. Restriction endonucleases were chosen from the restriction sites in the multiple cloning site (MCS) of the chosen vector that would result in the chosen construct and would not recognise any sequences within the gene.

The construct chosen for initial expression trials was insertion of the gene into the expression vector pET30a (Novagen, Inc.) with a C-terminal hexahistidine tag. Expression of recombinant proteins in the pET plasmids is controlled by the T7 promoter. This enables tightly controlled high-level expression in *E.coli* (Studier and Moffatt 1986). The construct was prepared by inserting the chloride channel genes between the *Nde* I and *Not* I cutting sites in the MCS of pET30a (see figs.2.3 and 2.4). Primers were designed that matched the first 27 bases of the 5' end of the gene (forward primer) and the last 24 bases of the 3' end (reverse primer). They also contained cutting sites for *Nde* I and *Not* I respectively. The primers also include extra bases flanking the endonucleases sites that increase the efficiency of the enzyme.

Forward Primer:

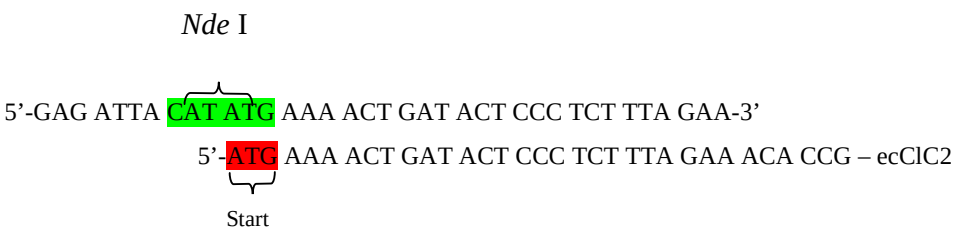

Reverse Primer:

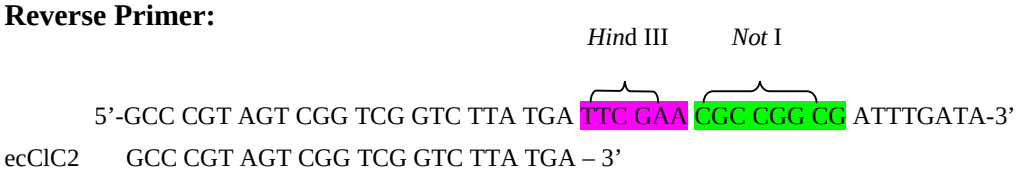

Fig. 2.2. Forward and reverse primers for the PCR of the ecClC2 gene. The primers are shown above the region of the gene to which they correspond . Restriction endonuclease recognition sites are highlighted. The *Hin*d III site was inserted for insertion of tags but was not used.

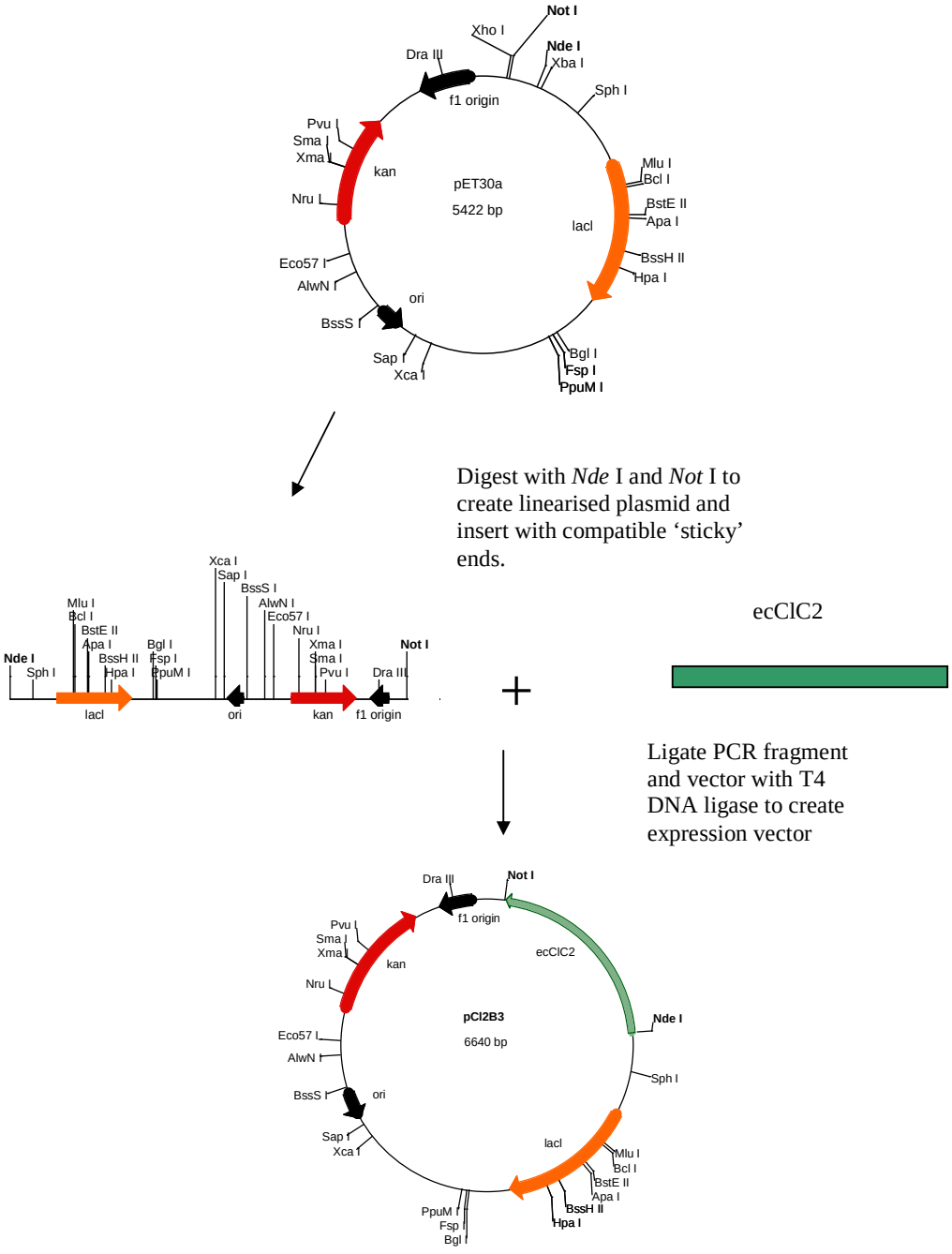

Fig. 2.3. Schematic of cloning strategy (see Sections 2.3, 2.4, 2.5 and 2.6). The ecClC2 gene is copied using PCR, creating the gene with two restriction endonuclease recognition sites (*Nde* I and *Not* I). The plasmid vector and PCR product are digested using these enzymes, linearising the vector and creating compatible DNA overhangs (sticky ends). The two digested products are mixed in a range of molar ratios and incubated with T4 DNA ligase to create an expression construct. Key: kan – kanamycin resistance gene; lacI – lac repressor gene; ori – origin of replication.

2.4 Initial PCR of ecClC1 and ecClC2 genes from *E.coli* genomic DNA.

Primers were synthesised by Sigma-Genosys, Ltd to 0.02µM scale and desalted. All PCR reactions were run in an iCycler™ thermal cycler (Biorad Laboratories) in 250µl thin walled tubes (Biorad Laboratories) with a final volume of 50 µl. The DNA polymerase used was *Pwo* polymerase (Thermo Hybaid, U.K). This thermophylic polymerase from *Pyrococcus woesei* has 3'-5' exonuclease activity (proof reading) introducing fewer mutations into PCR products. The reaction contents are shown in table 2.1.

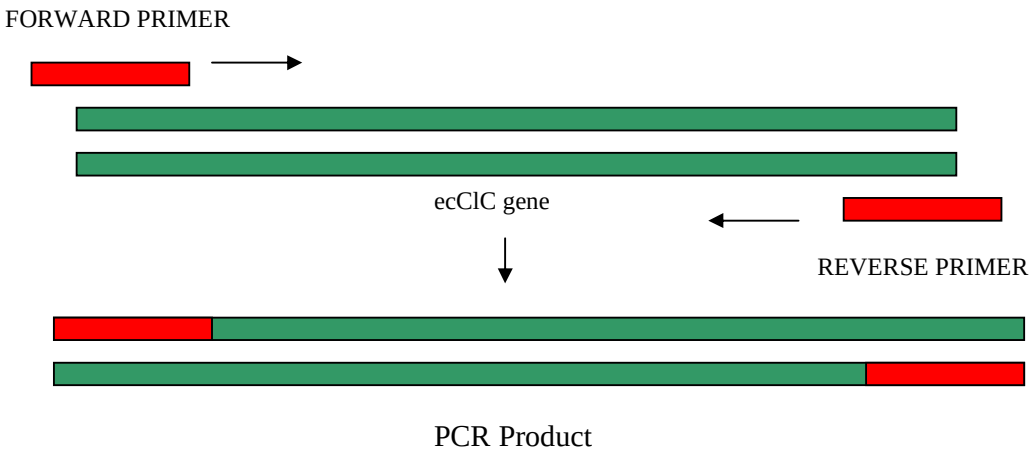

Fig. 2.4. Schematic of PCR. Primers (red) anneal to complementary sections of target gene (green). DNA polymerase then copies the gene (in the direction of the arrows) using the primer as a starting point.

	PCR Reaction Conditions for ecClC1	PCR Reaction conditions for ecClC2
Component	Amount (µl)	Amount (µl)
10x *Pwo* PCR reaction buffer	5	5
Nucleotide mix	1	1
Forward primer	5.6µl of 100 µg/ml stock (1µM)	5.7µl of 100 µg/ml stock (1µM)
Reverse primer	7.0µl of 100 µg/ml stock (1µM)	7.0µl of 100 µg/ml stock (1µM)
Template	1µl *E.coli* K-12 genomic DNA	1µl *E.coli* K-12 genomic DNA
Pwo polymerase	0.5	0.5
ddH_2O	29.9	29.8
Total	50	50

Table 2.1. PCR reaction conditions for ecClC1 and ecClC2.

The PCR reactions were run under the following conditions in the thermal cycler:

1. 97°C for 2:00 minutes – denaturing
2. 95°C for 0:30 seconds – denaturing
3. 65°C for 0:20 seconds – annealing
4. 72°C for 1:00 minutes – extension

} x5

then:

1. 95°C for 0:30 seconds – denaturing
2. 65°C for 0:20 seconds – annealing
3. 72°C for 1:30 minutes – extension

} x5

until an extension time of 4:30 minutes is reached.

The five repeat cycle of denaturation, annealing and extension was repeated eight times, after each round the extension time was increased by thirty seconds. The template DNA (in this case *E.coli* K-12 genomic DNA) is denatured to single strands by heating to 95°C, the drop in temperature to 65°C anneals the primers to the complementary regions in the template DNA. The extension temperature of 72°C is the optimum operating temperature for *Pwo* DNA polymerase and it is at this stage of the cycle that it copies the DNA. At the end of the run the temperature was ramped down to 4°C overnight.

The result of the PCR is shown in Fig. 2.5. The expected size of the products was 1300bp for ecClC1 and 1422bp for ecClC2. The PCR for ecClC1 shows a strong band between the 1000 and 1500bp markers, the lanes from the ecClC2 reactions show no product. The lanes containing the reactions from ecClC1 also contain non-specific bands from where the primers annealed to areas that are partially complimentary in the template.

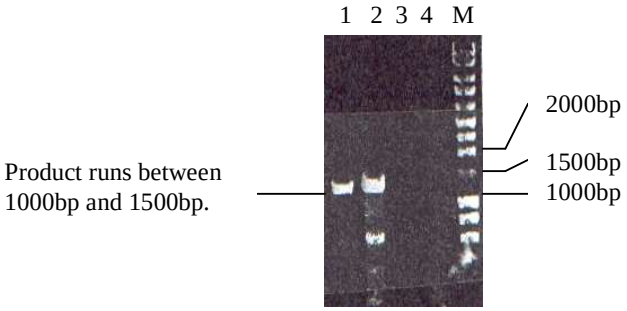

Fig. 2.5. 1% agarose gel stained with ethidium bromide for 30 minutes. M – DNA ladder (fragments are of known size (base pairs) and quantity); lanes 1 and 2 – PCR of ecClC1; lanes 3 and 4 – PCR of ecClC2, no product is present.

2.5 Optimisation of PCR conditions.

Several factors can be varied in PCR to optimise the production of a single product. These factors include: Annealing temperature, disruption of any secondary structure in the primers and magnesium concentration (alters the activity of the polymerase; this was not varied in this section but was used in Section 2.10.2)

The first factor to be altered was the annealing temperature. Both reactions were run as before (Table 2.1) but were run on a touchdown protocol. This led to many more non-specific products in the ecClC1 reaction and only non-specific products in ecClC2 (Fig.2.6). In this protocol, as each cycle is completed the annealing temperature is reduced by 1°C. As this was not successful, various ways of reducing primer secondary structure were used. Two methods were tried: First betaine, a substance that disrupts DNA secondary structure, was added to the reactions, two different concentrations of 1.5M and 3M were investigated. Secondly, the tubes and contents were heated to 95°C for five minutes to break any internal hydrogen bonds forming in the primers. The results are shown in figure 2.6. The addition of betaine was ineffective, but heating prior to the reaction was successful, as a clear band was observed at approximately 1500bp.

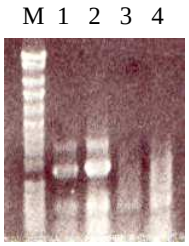

Fig. 2.6. 1% agarose gel stained with ethidium bromide for 30 minutes. M – Markers; lanes 1 and 2 – ecClC1 PCR run on the touchdown protocol; lanes 3 and 4 – ecClC2 PCR run on the touchdown protocol.

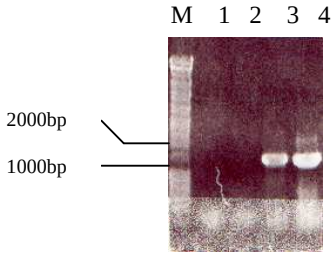

Fig. 2.7. 1% agarose gel stained with ethidium bromide for 30 minutes. M – Markers; lane 1 – ecClC2 PCR with 1.5M betaine; lane 2 – ecClC2 PCR with 3M betaine; lane 3 – ecClC2 PCR with a 10 minute hot start at 95°C; lane 4 – ecClC1 PCR product.

2.6 Production of an expression construct

In order to produce protein from the cloned DNA, the gene must be inserted into an expression plasmid. This section describes the insertion of the cloned genes into pET30a, a plasmid vector that allows high level protein expression in *E.coli* (Section 2.3).

2.6.1 Restriction endonuclease digestions.

Once the PCR conditions had been optimised, the successful reactions for both ecClC1 and ecClC2 were repeated. When the reactions were complete the PCR

products were purified from excess primers and enzymes using the QIAquick PCR product purification kit (Qiagen). After purification the products were stored at –20°C in 50µl of ddH_2O. The PCR products and pET30a vector DNA were digested with the restriction endonucleases *Nde* I and *Not* I. This created both 5' and 3' 'sticky' ends for ligation of the PCR products into pET30a. PCR and vector DNA was digested in the recommended buffer for the restriction enzyme (see Table 2.2 for reaction details). After each digestion the presence and extent of digestion was monitored by agarose gel electrophoresis, products were then purified using the QIAquick PCR product purification kit (Qiagen). After the DNA had been digested by both enzymes the samples were run on a 0.7% agarose gel to assess the amounts (Fig. 2.8). This was achieved by comparing the relative intensities of the bands to those in the DNA ladder that are of known quantity (see biological methods appendix, Section A.1). From this an approximate concentration was obtained for the plasmid and PCR DNA.

Sample	ecClC1	ecClC2	pET30a	Reaction Conditions
DNA	50 µl	50 µl	50 µl	37°C for 3.5 hours
Buffer	6 µl Roche H	6 µl Roche H	6 µl Roche H	
Not I‡	6 µl	6 µl	6 µl	
ddH_2O	16 µl	16 µl	16 µl	
Total Volume	80 µl	80 µl	80 µl	
DNA	50 µl	50 µl	50 µl	30°C overnight
Buffer	6 µl NEB† 4	6 µl NEB† 4	6 µl NEB† 4	
Nde I†	4 µl	4 µl	4 µl	
Total Volume	60 µl	60 µl	60 µl	

Table 2.2. Reaction conditions for restriction enzyme digests. Reaction buffers were supplied with the enzymes.

‡ Roche Diagnostics Ltd.
†New England Biolabs (UK) Ltd.

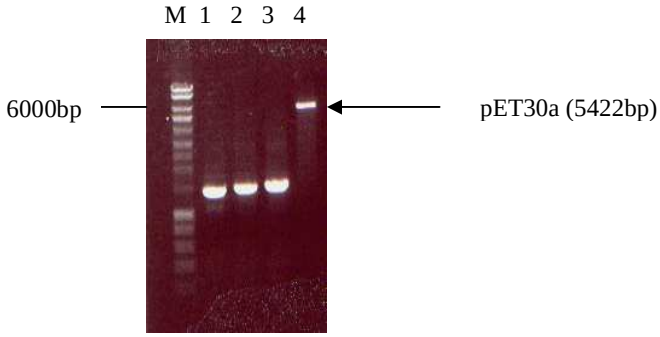

Fig. 2.8. 0.7% agarose gel stained with ethidium bromide for 30 minutes. M – markers; lane 1 – ecClC1 PCR product doubly digested; lanes 2 and 3 – ecClC2 PCR product doubly digested; lane 4 – pET30a doubly digested.

2.6.2 Ligations

Doubly digested (5' and 3') PCR products and plasmid vector were mixed in three different molar ratios: 1:1, 2:1 and 3:1 respectively (to a final volume of 8 µl made up with ddH_2O) with the amount of vector fixed at 100ng. Once mixed the reactions were heated to 45°C for five minutes and then cooled rapidly to 4°C. This reduced the number of religated vectors by reducing hydrogen bonds formed between vector 'sticky ends'. In theory, religation is not possible between different restriction sites; however, insertion of the gene did not occur until this step was introduced. Once the reactions were cooled, 1 µl T4 DNA ligase and 1 µl T4 DNA ligase 10x buffer were added (to a final volume of 10 µl). The reactions were left at room temperature overnight. Once complete the reactions were stored at 4°C. The reaction will produce plasmids either with the insert present or without. In order to separate and propagate these plasmids some of the ligation reaction was used to transform a DNA manipulation strain of *E.coli.* Colonies will grow from single transformants enabling the plasmids to be screened for those that contain the correct insert, using the following protocol.

The ligation reactions were diluted to 60 µl with 50 µl of ddH_2O to reduce the toxicity of the mixture to the DNA manipulation strain of *E.coli.* The host for transformation was NovaBlue ultra competent *E.coli* (Novagen, Inc.). NovaBlue cells were transformed with 5 µl of the diluted ligation reactions and plated out onto kanamycin autoselective LB agar plates. The plates were incubated at 37°C overnight. Six colonies from each plate were picked and used to inoculate 5ml

cultures of LB broth containing 50μg/ml kanamycin. Cultures were grown overnight at 30°C. Cells were harvested by centrifugation and plasmids were isolated using QIAquick plasmid mini-prep kit (Qiagen). To ascertain whether the purified plasmids contained an insert, a sample of each plasmid was digested with *Hin*d III (25°C 3 hours) to linearise the DNA. The samples were then run on a 0.7% agarose gel. Plasmids containing an insert do not migrate as far as empty plasmids. As an extra test the plasmids that were of a greater molecular weight were used as the template in PCR reactions with the conditions shown in Table 2.1. The result is shown in Fig.2.9. A product at approximately 1500bp was present after PCR showing the inserts were the ecClC channels. These plasmids were sequenced and the inserts matched the published sequences for the *E.coli* ClC genes (Blattner *et al.* 1997). Two plasmids that carried the ecClC1 gene and two that carried the ecClC2 gene were used to transform DH5α. Cultures were grown from transformed colonies and purified using Qiaquick plasmid miniprep kit (Qiagen).

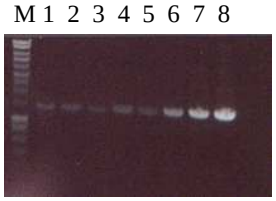

Fig. 2.9. 0.7% agarose gel stained with ethidium bromide for 30 minutes of PCR reactions using plasmids that appeared to contain inserts; all plasmids used as template contain the insert as a product is formed at 1500bp. M – Markers; lanes 1 to 4 - ecClC1 containing plasmid; lanes 5 to 8 – ecClC2 containing plasmids.

2.7. Test expression

2.7.1. Cell growth

The expression strain of *E.*coli, JM109 (DE3) was transformed with the two plasmids bearing the genes for the *E.coli* chloride channels. JM109 (DE3) contains the gene for T7 DNA polymerase in its genome. This is necessary for expression of a protein under the T7 promoter system in pET vectors. Cells from single colonies were used to inoculate 5ml cultures of LB broth. The cultures were grown at 37°C

until they reached an OD_{600} of approximately 1. These starter cultures were used to inoculate 1l of TB broth. The amount of pre-culture used followed the rule: for an OD_{600} of 0.2 add 10ml of pre-culture (equivalent to a 1000-fold dilution). Accordingly 1ml of pre-culture at an OD_{600} of 1 was added to 1l of TB broth. The cultures were grown to an OD_{600} of 1.0 for increased cell density, at this stage expression of the chloride channels was induced by addition of 0.5mM IPTG. The cultures were then left to grow at 37°C. After 3 hours the cells were harvested in a Beckman J-20 centrifuge at 5000rpm for 20 minutes. The supernatant was discarded and the cell pellets were stored at 4°C.

2.7.2. Purification

Each cell pellet was resuspended in 20ml resuspension buffer (50mM Tris pH 8.0; 200mM KCl; and complete protease inhibitor cocktail (Roche Diagnostics Ltd.)). The cells were lysed and the DNA broken down by running the cells twice through a high-pressure homogeniser (Glen Creston). During homogenisation 0.5ml PMSF (serine protease inhibitor, 10mM in isopropanol) was added drop-wise to the cells. Zwitergent $_{3\text{-}12}$ (a zwiterionic detergent) was added to the lysed cells, at a concentration of 40mM, and shaken gently for 30 minutes to solubilize the membrane proteins from the native *E.coli* membranes. After solubilization the samples were centrifuged at 18,000rpm for 30 minutes in a Beckman J-20 centrifuge to pellet insoluble material. The supernatant was collected and 1ml of Talon™ metal (cobalt) affinity resin (Clontech, U.K) was added. The sample was then shaken gently for 30 minutes to allow the resin to bind to the hexa-histidine (His_6) tagged proteins. After incubation with the Talon™ resin the sample was poured into a chromatographic column and the flow through collected. The resin was then washed with 20ml of buffer I and then 20ml buffer II (see Table 2.3). The second wash buffer contained 10mM imidazole and a higher salt concentration to remove non-specifically bound proteins. To elute the protein from the resin, 5ml of buffer III was added. Buffer III contained 200mM imidazole which is sufficient to displace most of the protein coordinated to the cobalt ions. Fractions of 0.5ml of the eluant were taken and samples were run on 12.5% SDS-PAGE gels. The result of these test expressions is shown in Figures 2.10 and 2.11. From the SDS-PAGE gels it can be seen that ecClC1 was not expressed, however ecClC2, was expressed to a high level.

Component	Buffer I	Buffer II	Buffer III
Tris pH 8.0	50mM	50mM	50mM
KCl	200mM	500mM	200mM
Zwitergent $_{3\text{-}12}$	10mM	10mM	10mM
Imidazole	0mM	10mM	200mM

Table 2.3. Components of the wash and elution buffers in the test expressions of the *E.coli* chloride channels.

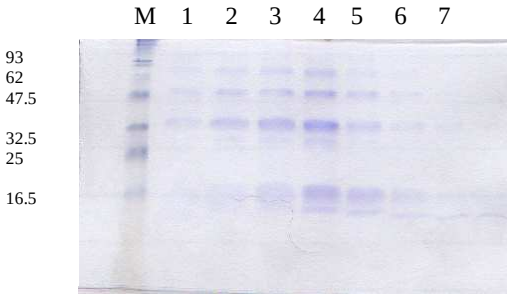

Fig. 2.10. 12.5% SDS-PAGE gel of the 8 fractions collected from the 200mM imidazole wash after expression of ecClC1. It can be seen from the gel that expression of ecClC1 is observed, however, many bands are seen, this may be due to proteolysis of the protein.

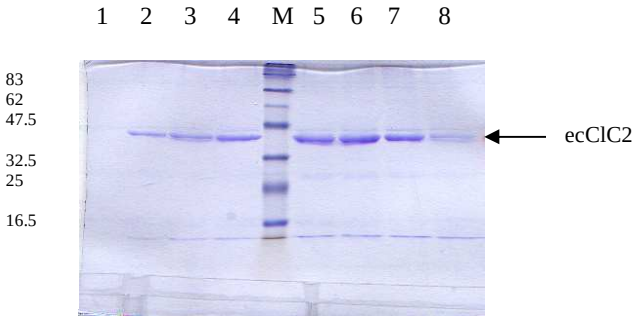

Fig. 2.11. 12.5% SDS-PAGE gel of the 8 fractions collected from the talon resin showing a high level expression of ecClC2. M – Molecular weight markers, molecular weight is marked on the left in kDa. Lanes 1 to 8 – fractions 1 to 8 from the 200mM imidazole wash. The protein runs between the 32.5 and 47.5kDa markers; this is smaller than the predicted 50kDa monomer. The size difference is due to fact that SDS is a detergent, thus the gel provides a native-like environment and the protein will remain folded to a certain extent, therefore migrating further through the gel than a denatured protein.

Several clones containing the ecClC1 gene were tested for expression with no success. It was therefore decided to continue with ecClC2 only, as the plasmid pCl2B3 demonstrated a very good level of expression as judged by Bradford assay SDS-PAGE and absorption at 280nm.

2.8. Initial optimisation of expression of ecClC2

There are many factors that affect the level of expression of a recombinant protein and these can be varied until the highest level of expression is achieved. This is particularly important with membrane proteins, as generally the levels of expression for membrane proteins can be ten fold lower than soluble proteins.

2.8.1. Strength, length and duration of expression

The first factors to be tested were the length of induction, the temperature and the concentration of IPTG. These factors affect the rate of production of the protein and may prevent toxicity of the product to the cells.

Cell cultures were grown as before but after induction the temperature was reduced to 30°C or 25°C and the cells were left to grow overnight. After purification as before it was found that ecClC1 was expressed but was still susceptible to proteolysis and expression of ecClC2 was similar but with more impurities found in the eluant. As the expression of ecClC2 was acceptable at 37°C the culture was induced and left at 37°C for 6 hours. This gave the best expression in terms of amount of protein and initial purity.

The concentration of IPTG was varied, from 0.25mM to 0.75mM in steps of 0.25. Induction with 0.25mM IPTG gave the best levels of expression.

2.8.2 Cell Lines

Three *E.coli* cell lines were tested for expression of ecClC1 and ecClC2: JM109 (DE3), BL21 (DE3) and C41 (DE3). C41 cells have been developed for expression of membrane and toxic proteins (Miroux and Walker 1996). Each cell line was transformed as before and 1l cultures were used and purified as before. The fractions were run on 12% SDS-PAGE gels and assayed for quantity using the Bradford assay and by absorption at 280nm (OD_{280}). The SDS gels are shown in

Figure 2.12 to 2.14. It can be seen from these results that BL21 (DE3) shows the highest expression of ecClC2 (2.6mg/litre culture), then C41 (DE3) (2.25mg/litre culture) and finally JM109 (DE3) (2.15mg/litre culture). However, in terms of the number of contaminants that co-elute from the cobalt resin, the order is reversed. In BL21 (DE3) there is a pair of contaminants at approximately 25kDa that is absent in JM109 and barely perceptible in C41. Therefore, C41 (DE3) was chosen as the initial expression strain as a balance between level of expression and level of contaminants.

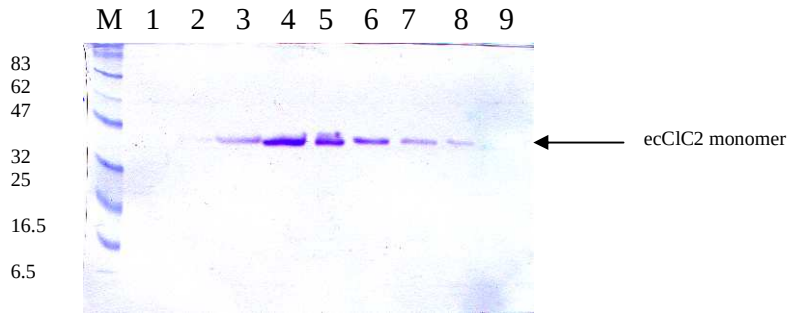

Figure 2.12. SDS-PAGE gel of fractions of ecClC2 expressed in JM109 (DE3) cells and solubilised in decylmaltoside. M - molecular weight markers; 1-9 – fractions 1-9 from the Talon™ cobalt column. Molecular weights of the markers are shown to the left of the gel in kDa.

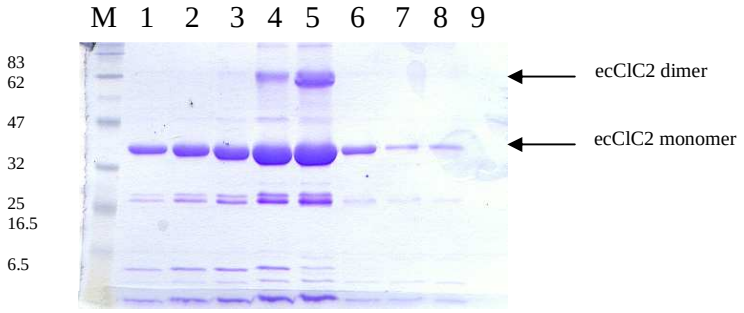

Figure 2.13. SDS-PAGE gel of fractions of ecClC2 expressed in BL21 (DE3) cells and solubilised in decylmaltoside. M - molecular weight markers; 1-9 – fractions 1-9 from the Talon™ cobalt column. Molecular weights of the markers are shown to the left of the gel in kDa. In this gel ecClC2 dimer can be seen; this is probably due to the amount of protein present. SDS is a harsh detergent that will disrupt the interaction that forms the dimer. However, it is believed that there is a sufficient excess of ecClC2 that not all of the protein is reduced to monomer.

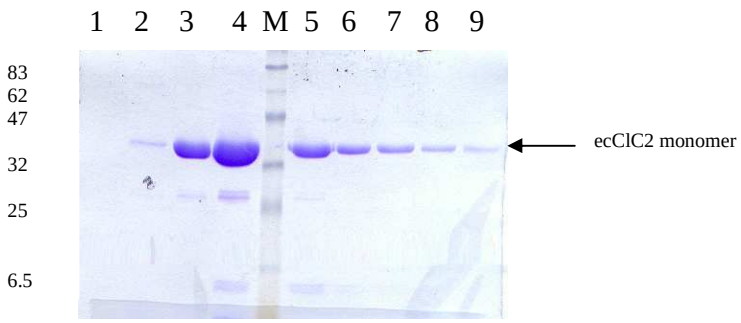

Figure 2.14. SDS-PAGE gel of fractions of ecClC2 expressed in C41 (DE3) cells and solubilised in decylmaltoside. M - molecular weight markers; 1-9 – fractions 1-9 from the Talon™ cobalt column. Molecular weights of the markers are shown to the left of the gel in kDa.

2.8.3.Detergents

2.8.3.1 Detergent for extraction

The choice of detergent in the purification of membrane protein affects the amount obtained and the stability of the protein enormously (Ostermeier and Michel 1997). The ideal detergent for solubilisation of membrane proteins is one that is gentle on the protein, removes most of the protein from the native membrane and is relatively inexpensive. The detergent used for the test expressions was zwitergent $_{3\text{-}12}$. In conjunction with testing cell lines (Section 2.8.2) the detergent *n*-Decyl-β-D-thiomaltoside (decylmaltoside) (Anatrace) was tested. Decylmaltoside is an uncharged detergent with a sugar (maltose) hydrophilic head and 10-carbon hydrophobic tail. It was found to extract ecClC2 very well from the membrane and produce a clean sample of protein that was stable for many weeks at room temperature.

2.8.3.2 Detergent used for further experimentation

The choice of detergent for further purification and subsequently crystallisation must also be tested. Seven detergents were tested to see if ecClC2 was stable in them. Seven 1 litre cultures were grown in the manner described in 2.6.1 and purified as in 2.6.2, solubilising in Zwitergent $_{3\text{-}12}$. However, in the wash buffers the detergent was changed, thereby exchanging the detergent while the protein is bound to

the cobalt resin. The detergents tried were: Thesit; Octylglucoside; Decylglucoside; Dodecyldimethylglycine, Lauryldimethylamine N-oxide (LDAO); Anapoe $C_{10}E_8$ and Anapoe $C_{12}E_8$ all at concentrations well above the critical micelle concentration (CMC). The fractions transferred to octylglucoside and decylglucoside both precipitated immediately after elution from the column, the other sample appeared to remain soluble. However, when the fractions were analysed by SDS-PAGE, only the fraction solubilised in LDAO contained ecClC2. Out of the detergents tested, three remained as candidates: DM, Zwitergent $_{3\text{-}12}$ and LDAO.

2.8.4 Media

The choice of medium can also make a difference to the level of expression of recombinant proteins. Three media were tested: Terrific Broth (TB), Super Broth (SB) and Luria-Bertani (LB). SB and TB are much richer media than LB and cells grown in this media showed better expression than LB as a higher cell density was reached providing more cells in which to express ecClC2. Of these two TB was the better as it contains a phosphate buffer maintaining the pH thereby keeping the environment at the optimum for the cell.

2.9 Construction of new expression clones with protease sites to remove the hexa-histidine tag.

Once ecClC2 could be produced to high enough levels to enable structural studies, new clones were designed to enable the His_6 tag to be removed. This produces a protein closer to the wild type than if the tag was left intact.

2.9.1. Choice of protease sites

Three protease sites were chosen and clones made concurrently as it was unknown which protease would be the best at removing the his tag in this construct. The proteases were thrombin, the 3C protease from Rhinovirus and TEV protease from Tobacco etch virus. Thrombin is commercially available and expression clones for 3C and TEV were available in the laboratory.

2.9.2. Design of PCR primers

As the gene was to be put back into pET30a, only the reverse primers had to be changed to include the protease site, the original forward primer could be used. The new primers included 24 bases complementary to the ecClC2 gene, bases corresponding to the protease cleavage site (using *E.coli* optimised codons (Hale and Thompson 1998)) and restriction endonuclease sites. Two primers, for the 3C protease cutting site construct were designed, one with the cutting site, the other removes the last 4 amino acids from the protein that were predicted to be disordered from the secondary structure prediction program PHD (Rost and Sander 1993). The primers for insertion of the thrombin and TEV protease sites corresponded to the last 8 codons of the ecClC2 gene plus the cutting site and the restriction endonuclease site for *Xho* I to insert just before the His tag present in pET30a (Fig. 2.16).

2.10 PCR

2.10.1. PCR of 3C protease site containing product

PCR reactions were performed as in Sections 2.3 and 2.4 with some modifications. The reactions were run with 50μM of the primers with the same thermal cycler protocol except that the annealing temperature was 60°C. The result of the PCR reaction is shown in Figure 2.15.

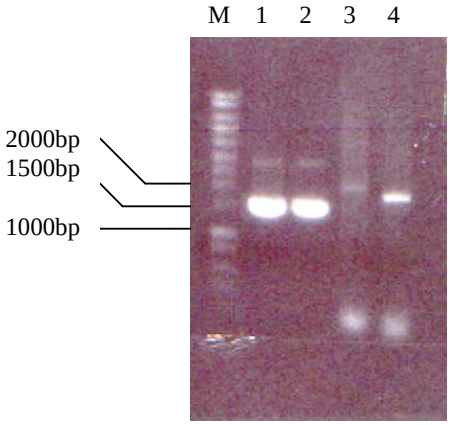

Fig. 2.15. 1% agarose gel of the PCR products to insert a 3C cutting site. M – DNA fragment ladder; lanes 1 and 2 PCR product of ecClC2 with a 3C recognition site; lanes 3 and 4 PCR reaction to form ecClC2 with a 3C cutting site without the last 4 amino acids SENT, some non-specific products are present in lanes 3 and 4.

3C Protease Primers:

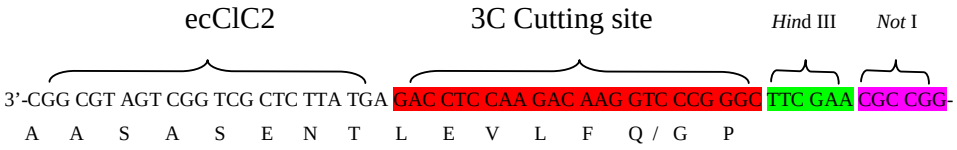

CGATTTGATA-5’

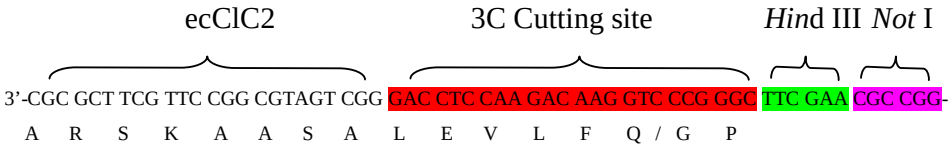

CGATTTGATA-5’

Thrombin primer:

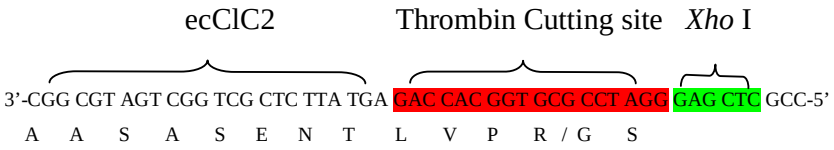

TEV primer:

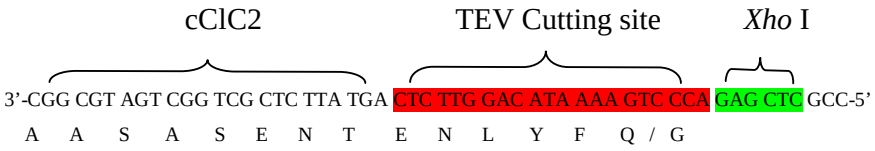

Fig. 2.16 Primers designed to include a 3C, thrombin and TEV protease cutting site in the protein product. The single letter amino acid code is shown beneath the codon to which it corresponds. 3C protease cuts between Q and G; thrombin cuts between R and G and TEV between Q and G as indicated by a forward slash.

From Fig 2.17 it can be seen that the PCR to produce the full length protein worked and the reaction to remove the last four amino acids S E N T failed.

2.10.2. Optimisation of PCR of product lacking SENT

Various conditions were then changed to optimise the PCR conditions. Treatments used to reduce any secondary structure in the primer proved ineffective. Reducing the annealing temperature to 40°C produced a product running to the correct size on an agarose gel (Fig. 2.17) although there are still non-specific products present. To reduce the number of non-specific products, the concentration of magnesium sulphate in the reaction buffer was varied. This changes the activity of the *Pwo* DNA polymerase and may lead the formation of a single product. The concentration of magnesium sulphate was varied from 1.5mM to 4mM in steps of 0.5mM. The reactions were run with an annealing temperature of 40°C. The results are shown in figure 2.17. Varying the magnesium concentration has reduced some of the non-specific products at 2.5mM. However, some are still present. Therefore the reaction containing 2.5mM magnesium sulphate was repeated 8 times and the reactions pooled. To remove the non-specific products the pooled reactions were run on a 1% agarose gel (Fig. 2.18). The band running to approximately 1500bp was excised from the gel and purified using an Agarose gel purification kit (Roche diagnostics, Ltd).

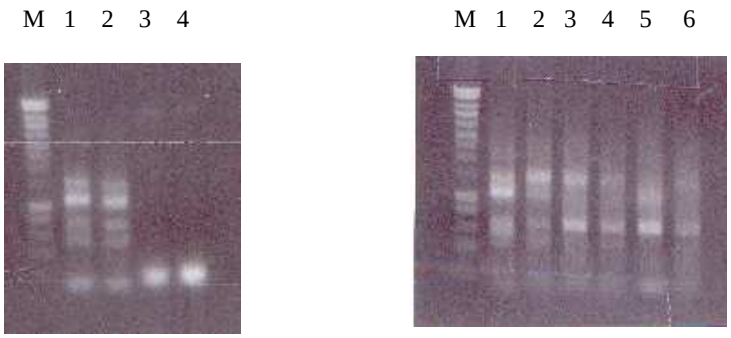

Fig. 2.17. 1% agarose gels of PCR reactions. Left: PCR reaction run with an annealing temperature of 40°C. Lane 1: 10 minute hot start (95°C); lane 2: 20 minute hot start; lane 3: 1.5M betaine; lane 4: 3M betaine. Right: PCR reaction varying $MgSO_4$ concentrations. Lane 1: 1.5mM $MgSO_4$; lane 2: 2mM; lane 3: 2.5mM; lane 4: 3mM; lane 5: 4mM; lane 6: 4.5mM.

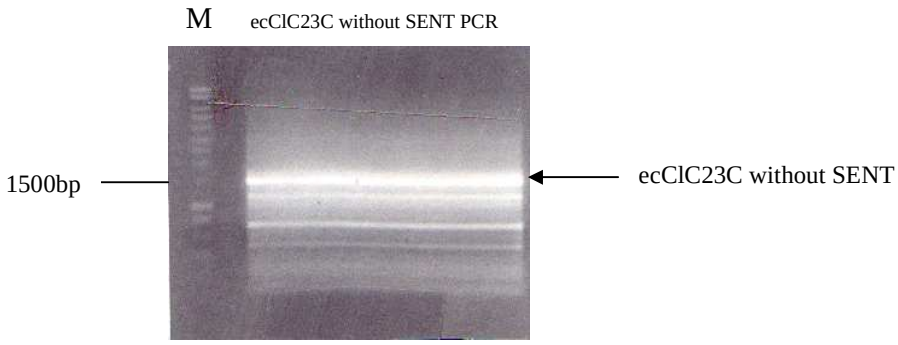

Fig. 2.18. 1% agarose gel containing the PCR product of interest (marked).

2.10.3. PCR of products containing a thrombin cutting site.

The PCR reactions for this construct were performed as before with an annealing temperature of 60°C. The reactions were successful but contained some non-specific products. Therefore the product was purified by gel extraction.

2.10.4. PCR of products containing a TEV cutting site.

The PCR reactions were performed as before with an annealing temperature of 60°C and were successful. The products were purified with the QIAquick PCR product purification kit (Qiagen).

2.11. Digestion and Ligation

The PCR reaction products were purified as described in Section 2.9. The products, and pET30a plasmid, were then incubated with *Nde* I and *Xho* I for the TEV and thrombin primers and *Nde* I and *Not* I for the 3C primer (Table 2.4). After digestion the products were mixed, with the appropriately digested pET30a, in a 3:1 molar ratio. Ligations were performed as in 2.5.2. Ligation reactions were diluted six fold in ddH_2O, of this 5µl was used to transform 50µl of NovaBlue competent cells. Single colonies were picked and grown in 5ml LB (50µg/ml kanamycin) overnight at 30°C. Cultures were then harvested by centrifugation and the plasmids purified using the QIAquick plasmid mini-prep kit (Qiagen). The plasmids were then tested for the

presence of the insert by digestion and detection of a gel shift or by using the plasmid as PCR template (Figures 2.19 and 2.20).

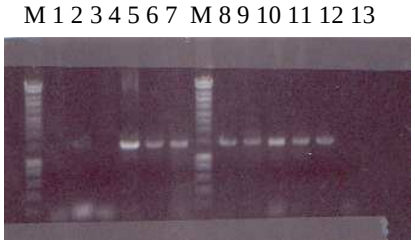

Fig.2.19. 1% agarose gel showing the PCR products using potential plasmids containing the insert as the template. Only plasmids containing the ecClC2 insert will produce a product at approximately 1500bp. Clones 5, 6, 7 8, 9, 10, 11 and 12 contain the ecClC2 gene as a product is observed.

Sample	ecClC2 3C	ecClC2 3C without SENT	ecClC2 TEV	ecClC2 Thrombin	pET30a	Reaction Conditions
DNA	50 µl	50 µl	50 µl	50 µl	50 µl	37°C for 3.5 hours
Buffer	8 µl Roche H	6 µl Roche H	6 µl Roche	6 µl Roche	6 µl Roche H	
Not I‡ or *Xho* I‡	6 µl *Not* I	2 µl *Not* I	4 µl *Xho* I	4 µl *Xho* I	6 µl	
ddH_2O	16 µl	2 µl	0 µl	0 µl	16 µl	
Total Volume	80 µl	60 µl	60 µl	60 µl	80 µl	
DNA	50 µl	50 µl	50 µl	50 µl	50 µl	30°C overnight
Buffer	6 µl NEB† 4	6 µl NEB† 4	6 µl NEB†4	6 µl NEB†4	6 µl NEB† 4	
Nde I†	4 µl	4 µl	4 µl	4 µl	4 µl	
Total Volume	60 µl	60 µl	60 µl	60 µl	60 µl	

Table 2.4. Reaction conditions for restriction enzyme digests. Reaction buffers were supplied with the enzymes.

‡ Roche Diagnostics Ltd.
†New England Biolabs (UK) Ltd.

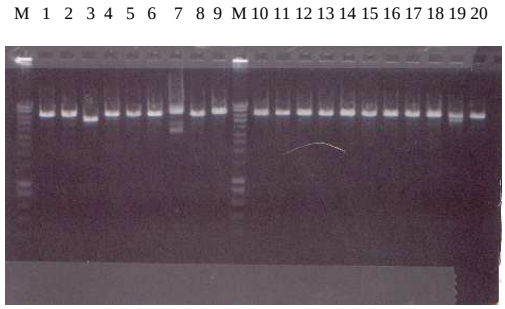

Fig.2.20. 1% agarose gel showing digested plasmids from colonies from the 3C with SENT construct. Plasmids were incubated with *Hin*d III (one cutting site) for 1 hour at 37°C. Plasmids with an insert do not migrate as far as those without an insert. Lanes 3, 7 and 19 do not contain an insert as the plasmids migrate further in the gel.

2.12. Test expressions

Two plasmids of each construct that contained an insert were selected for test expressions. The plasmids were transformed into an expression strain. Cultures were grown and the protein purified as in Section 2.6 using Zwitergent $_{3\text{-}12}$ as the extraction detergent. The results are shown in Figures 2.21 to 2.23. Clones that showed initial expression levels greater that 1mg per litre of culture (assessed by Bradford assay and OD_{280}) were judged to express enough protein for further study.

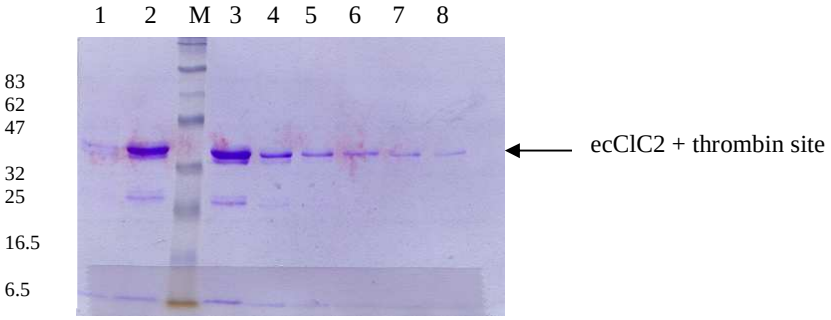

Fig. 2.21. SDS-PAGE gel of fractions from a test expression of ecClC2 with a thrombin protease cutting site upstream of the hexa-histidine tag.

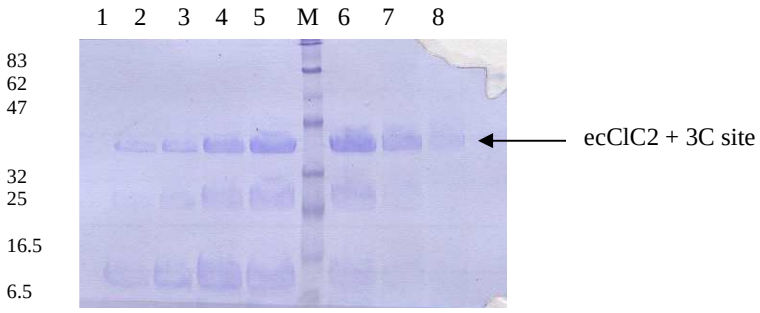

Fig. 2.22. SDS-PAGE gel of fractions from a test expression of ecClC2 with a 3C protease cutting site upstream of the hexa-histidine tag.

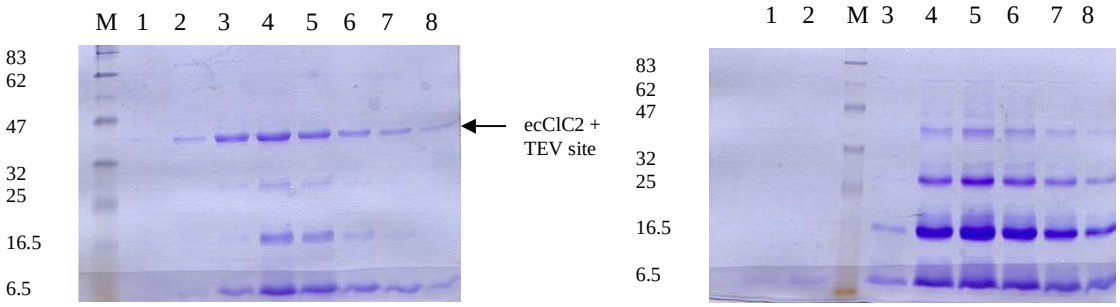

Fig. 2.23. SDS-PAGE gel from test expressions of ecClC2 with a TEV protease cutting site upstream of the hexa-histidine tag. The gel on the left shows fractions from a clone that expresses ecClC2 to a high level. The gel on the right shows many proteins that may be contaminants or products of proteolytic cleavage ecClC2TEV, this clone was abandoned.

Plasmids that showed good expression above 1mg per litre culture were sequenced to verify the presence of the ecClC2 gene, the cutting site and that no mutations had occurred during the PCR reaction.

2.13 Test Digestion of ecClC2thrombin construct.

As thrombin was available immediately, the ecClC2 thrombin construct was the first to be tested. Three 1l flasks of TB were grown and the protein purified as described in Section 2.6. The fractions were analysed for purity on a 12.5% SDS-PAGE gel and were found to contain few contaminants. The fractions were then

pooled and concentrated to 2mg/ml in a 30kDa molecular weight cut off centricon® 30 (Millipore). To this solution 1.15U (0.4U/mg protein) of restriction grade thrombin (Novagen, Inc.) was added. To maintain thrombin activity, calcium chloride was added, to a final concentration of 2.5mM. The reaction was left at room temperature for 2.5hours. After this time the protein was found to have precipitated. After a series of experiments it was found that the level of precipitation increases with the extent of digestion with thrombin. There is a possibility that removing the hexa-histidine tag interferes with dimer formation causing the protein to precipitate. It was then decided to abandon these constructs and try a new construct bearing an N-terminal hexa-histidine tag with a thrombin site.

2.14 Construction of an expression clone with an N-terminal hexa-histidine tag.

For this expression clone the plasmid vector pET28a was chosen as this plasmid has a hexa-histidine tag and a thrombin recognition sequence encoded.

2.14.1 Primers

The forward primer used for all the ecClC2 constructs was again used as there is an *Nde* I recognition site in pET28a. The reverse primer was designed to be complementary to the last 24 bases of the ecClC2 gene, it also included a stop codon and a *Xho* I recognition site for insertion into pET28a (Fig. 2.24).

N-terminal hexa-histidine tag reverse primer:

Fig. 2.24. Reverse primer for insertion of ecClC2 into pET28a.

2.14.2 PCR, digestion and ligation

The PCR reaction was run as in Section 2.3 with the following exceptions: The annealing temperature was 60°C and 5% formamide was added to disrupt the secondary structure of the primers, replacing the 95°C 10 minute hot start (see Table 2.5). The result is shown in Figure 2.25; a single product was produced. The product was purified and digested with *Nde* I and *Xho* I with pET28a vector (Table 2.6). Doubly digested PCR and vector DNA were purified and run on a 1% agarose gel, and the relative amounts of DNA judged as compared to the molecular weight standards (Fig. 2.25). Ligation reactions were performed as in Section 2.5.2. NovaBlue competent cells were transformed with a ligation reaction as before. Single colonies were picked and plasmids were tested for insert by PCR.

	PCR Reaction Conditions for ecClC2NTHis6
Component	Amount (µl)
10x *Pwo* PCR reaction buffer	5
Nucleotide mix	1
Forward primer	5.7µl of 100 µg/ml stock (1µM)
Reverse primer	5.5µl of 100 µg/ml stock (1µM)
Template	1µl *E.coli* K-12 genomic DNA
Pwo polymerase	0.5
Formamide	2.5
ddH_2O	28.8
Total	50

Table 2.5. PCR reaction conditions for ecClC2 with an N-terminal his tag.

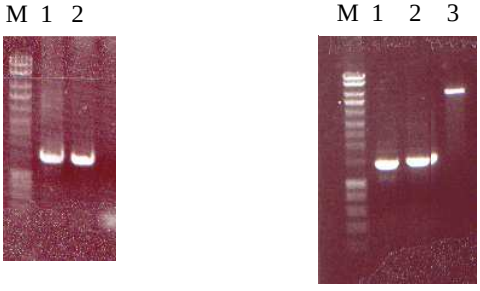

Fig.2.25. Left: Single products formed after PCR as in Table 2.5 run on a 0.7% agarose gel running to approximately 1500bp; M- molecular weight markers; lanes 1 and 2 – PCR products ecClC2. Right: Doubly digested PCR product (lanes 1 and 2) and pET28a plasmid vector (lane 3); M – molecular weight markers.

Sample	ecClC2NTH$_6$	pET30a	Reaction Conditions
DNA	50 µl	50 µl	37°C for 4.5 hours
Buffer	6 µl Roche H	6 µl Roche H	
Xho I[‡]	4 µl	4 µl	
Total Volume	60 µl	60 µl	
DNA	50 µl	50 µl	30°C overnight
Buffer	6 µl NEB[†] 4	6 µl NEB[†] 4	
Nde I[†]	4 µl	4 µl	
Total Volume	60 µl	60 µl	

Table 2.6. Reaction conditions for restriction enzyme digests to insert ecClC2 DNA into pET28a. Reaction buffers were supplied with the enzymes.

2.14.3 Test expression

Plasmids containing an insert were used to transform the expression strain BL21 (DE3). Cultures were grown and the protein purified as in Section 2.6 using Zwitergent $_{3\text{-}12}$ as the extraction detergent and expressing for 6 hours at 37°C. The fractions obtained from the cobalt affinity column were analysed by SDS-PAGE (Fig. 2.26). From the test expression it was seen that ecClC2 with an N-terminal His tag was expressed but only to a low level. The expression level obtained with this construct was below 1mg per litre of culture and therefore unsuitable for structural studies. It was therefore decided to revert to the original construct of a C-terminal His tag in the pET30a vector as this is the only clone that expresses up to 2.5mg per litre of culture.

[‡] Roche Diagnostics Ltd.
[†]New England Biolabs (UK) Ltd.

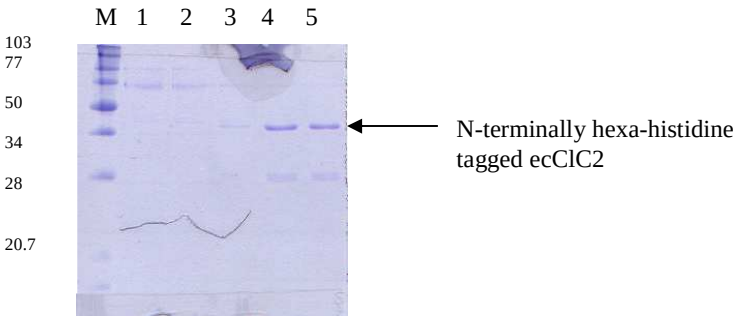

Fig. 2.26. 12% SDS-PAGE of fractions from test of expression of ecClC2 with an N-terminal His tag. M – molecular weight markers; lanes 1 to 5 fractions 2 to six from the 200mM elution from the metal affinity column.

2.15 Conclusions

Several expression constructs were created that produced recombinant ecClC2 to a high enough level for structural studies by X-ray crystallography. However, after problems with some of the constructs one emerged as a candidate for scale up expression, this was the plasmid referred to as pCl2B3. This construct produces ecClC2 with a C-terminal hexa-histidine tag. The scale up of expression, further purification and crystallisation of ecClC2 is described in Chapter 3.

CHAPTER 3:

CRYSTALLISATION OF ecClC2 AND X-RAY DATA COLLECTION

The crystallisation of a protein requires that a purity of at least 95% is achieved. This chapter describes the scale up of the expression system detailed in Chapter 2 and the further purification of ecClC2 to near homogeneity. The crystallisation and X-ray diffraction data collection from crystals is also reported.

3.1 Large-scale expression and purification of ecClC2

3.1.1 Transformations

C41 (DE3) or BL21 (DE3) cells (50µl) were transformed with 1 µl pCl2B3 and plated onto LB agar plates containing kanamycin (50µg/ml) to select for successful transformants. A single colony was picked and used to inoculate a 5ml culture of LB broth (50µg/ml kanamycin). The culture was incubated at 30°C in a shaker incubator overnight. The cultures' growth was monitored by the optical density at 600nm (OD_{600}).

3.1.2 Expression

The OD_{600} of the pre-culture was measured and the appropriate amount (10ml pre-culture to 1l for an OD_{600} of 0.2) added to 6 x 1l of TB (50 µg/ml kanamycin) in 4l baffled conical flasks. The flasks were placed in a shaker incubator at 37°C at 220rpm. The OD_{600} of the cultures was measured and were induced with 0.25mM isopropyl-β-D-thiogalactopyranoside (IPTG) at an OD_{600} of 1.0 to 1.2; 50 µg/ml kanamycin was then added to each of the flasks to maintain the presence of the plasmid. The flasks were then left at 37°C for six hours. The OD_{600} after a six hour expression usually reached a value of 2 to 3. The cultures were poured into 1l centrifuge pots and the cells harvested by centrifugation at 5000rpm for 20 minutes in a Beckman Avanti™ J-20 centrifuge at 4°C. The pelleted cells were placed on ice and

immediately resuspended in 100ml resuspension buffer (50mM Tris pH 8.0; 200mM NaBr; 0.4M glucose; protease inhibitor cocktail (Roche Diagnostics Ltd.)).

3.1.3 Initial purification

3.1.3.1 Solubilization of the membranes

The resuspended cells were lysed by four runs through a high pressure homogeniser (Glen Creston, Ltd). The pressure was maintained between 15 and 20kpsi; this was sufficient to lyse the cells and break down the DNA. During homogenisation, 1ml PMSF (10mM in isopropanol) was added drop-wise to the cells. As ecClC2 is an integral membrane protein, a considerable amount of its exposed surface is hydrophobic which in the membrane will be surrounded by *E.coli* lipids. In order to remove the protein from the lipids and to maintain its solubility in a hydrophilic environment, a detergent was added to a concentration in excess of the critical micelle concentration (CMC) for that detergent. The detergent's hydrophobic tails surround the hydrophobic areas of the protein. The hydrophilic headgroups are exposed to the aqueous environment, shielding the hydrophobic surfaces and thereby maintaining the solubility of the protein. Once lysed, the volume of the solution was measured and 20 to 30mM decyl maltoside (DM) added to solubilize ecClC2 from the native *E.coli* membrane. The solution was then stirred gently for 3 hours at room temperature to complete extraction. Insoluble material was removed by centrifugation at 18,000rpm for 30 minutes at 4°C in a Beckman Avanti™ J-20 centrifuge. The supernatant was decanted into a glass bottle.

3.1.3.2 Metal affinity chromatography

Talon™ metal (cobalt) affinity resin (Clontech, U.K) was equilibrated with buffer I and resuspended in 10ml supernatant. This suspension was then added to the remaining supernatant and shaken gently for 1 hour at room temperature to bind the His_6 tagged ecClC2 to the resin.

After binding, the solution was poured into a 2.5cm diameter 20cm long low-pressure chromatography Econo-column (Bio-Rad Laboratories, Ltd.). The resin was retained in the column and an aliquot of the flow through was taken for analysis by SDS-PAGE. The resin was then resuspended in 50ml buffer I. The buffer was then

drained off, leaving the resin in the column. Again, an aliquot of the flow-through was retained for analysis. At this stage a flow adapter was fitted to the column and attached to a peristaltic pump (Anachem, Ltd.). The bottom of the column was attached to an Econo UV monitor (Bio-Rad Laboratories, Ltd.) to observe the presence of protein by absorption at 280nm (OD_{280}); the absorbance was monitored with a chart recorder (Fig. 3.1). The detector was also connected to a fraction collector set to collect fractions of 2ml. The resin was then washed by pumping 50ml buffer I through the column at a flow rate of 1ml/min; after this wash the OD_{280} had reached zero. The resin was then washed with 100ml buffer II. Buffer II contained 10mM imidazole and 1M NaBr (see Table 3.1), and these components removed most of the non-specific contaminants bound to the column. 30ml buffer III was passed down the column to return the salt concentration to 200mM.

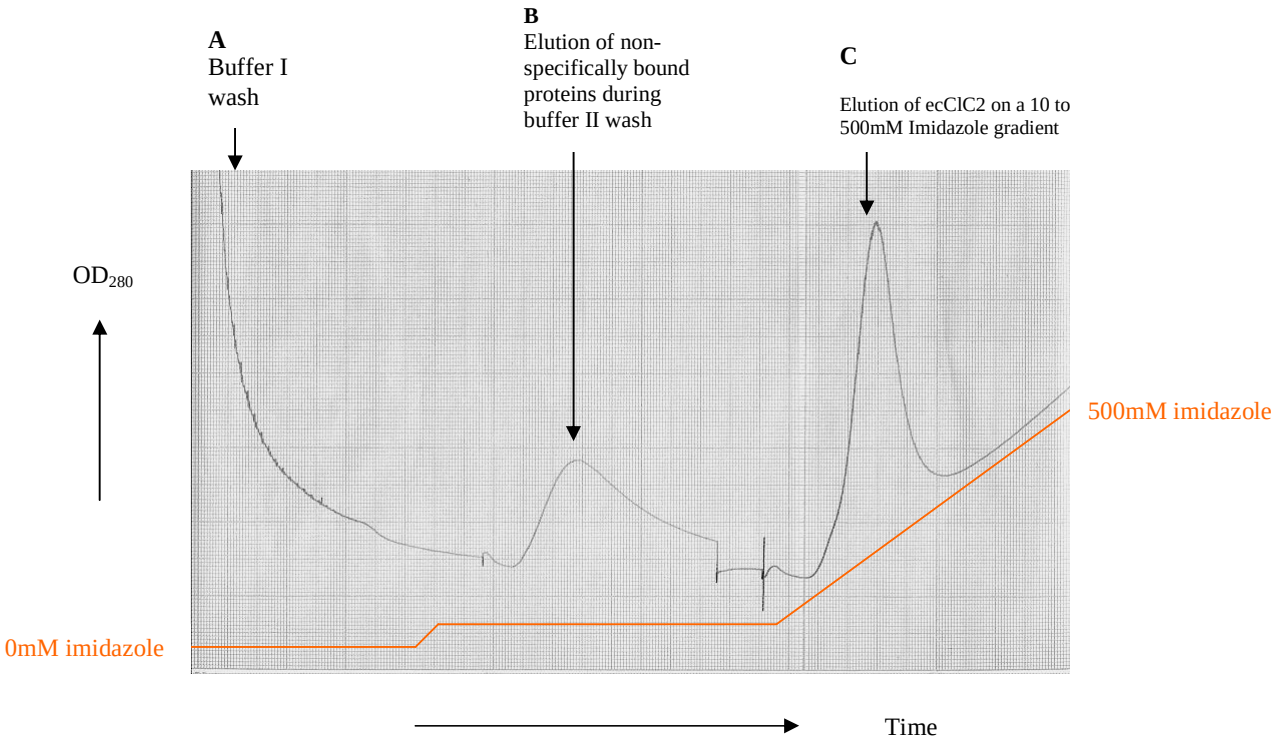

Fig. 3.1 Chromatogram showing the purification of ecClC2 from solubilized *E.coli* membranes. **A:** As buffer I is pumped over the column the OD_{280} reaches zero as non-binding proteins are washed off the resin. **B:** The high salt concentration and 10mM imidazole in buffer II displaces loosely bound proteins from the resin. **C:** The imidazole gradient reaches a sufficient concentration to elute ecClC2 from the affinity resin. The relative concentration of imidazole is shown by the red line. The OD_{280} increases with the gradient as imidazole absorbes at 280nm. See Fig. 3.2 for SDS-PAGE analysis of A,B and C.

A gradient was then formed between 20ml buffer III and 20ml buffer IV ramping from 10mM to 500mM imidazole. Fractions of 2ml were collected while the gradient was running and the fractions collected during ecClC2 elution were marked (Fig. 3.1). The aliquots retained for analysis from the previous wash steps and the fractions containing ecClC2 were analysed by SDS-PAGE to assess the loss of ecClC2 during purification and the purity of the eluted protein; the results are shown in Figure 3.2.

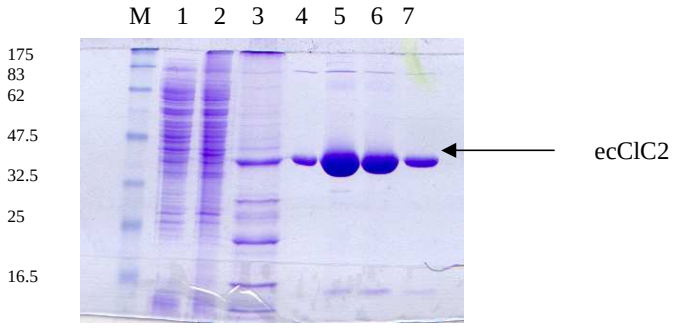

Fig. 3.2 12% SDS-PAGE gel; the protein was visualised by coomassie blue stain, molecular weights of the markers are shown to the left of the gel in kDa. M – molecular weight markers; 1 – First flow through from binding protein to affinity resin; 2 – First wash with buffer 1 (**A** in Fig. 3.1); 3 – Buffer II wash (**B** in Fig. 3.1); 4 to 7 – fractions 5 to 8 from the imidazole elution (**C** in Fig. 3.1).

From the SDS-PAGE analysis of the purification (Fig. 3.2) it can be seen that ecClC2 is lost at all stages of the purification, particularly in the buffer II wash. This loss is acceptable given the high level of purity achieved in one step. The yield from the initial purification was found to be 2 to 2.5mg/litre culture as assessed by Bradford assay and absorbance at 280nm.

3.1.4 Dialysis

The fractions containing ecClC2 were pooled. Spectra/Por® 30,000Da molecular weight cut off dialysis membrane (Fischer Scientific UK, Ltd.) was rinsed in deionised water and soaked in buffer V. The pooled fractions from the cobalt resin were gently pipetted into the dialysis membrane, all bubbles were removed and the

tubing was sealed at both ends. The tubing was then placed in 150ml of buffer V and left overnight at room temperature while stirring gently. This step removed the high concentration of imidazole present in the fractions.

Component	Buffer I	Buffer II	Buffer III	Buffer IV	Buffer V
Tris pH 8.0	50mM	50mM	50mM	50mM	50mM
NaBr	200mM	1 M	200mM	200mM	200mM
DM or LDAO	10mM	10mM	10mM	10mM	5mM
Imidazole	0mM	10mM	200mM	500mM	0mM

Table 3.1 Components of the buffers used in the purification of ecClC2.

3.1.5 Gel filtration chromatography

Gel filtration or size exclusion chromatography was performed on a Bio-Sil SEC 250 silica based column (Bio-Rad laboratories, Ltd) run on a BioLogic HR system (Bio-Rad laboratories, Ltd). The SEC 250 column was equilibrated with 50ml buffer V and the protein was removed from the dialysis tubing and concentrated to approximately 4mg/ml in a centriprep® 30 (Millipore). Protein was injected onto the column in 0.5ml aliquots and run at a flow rate of 1ml/minute with buffer V. The elution profile was monitored by absorbance at 280nm (Fig 3.3).

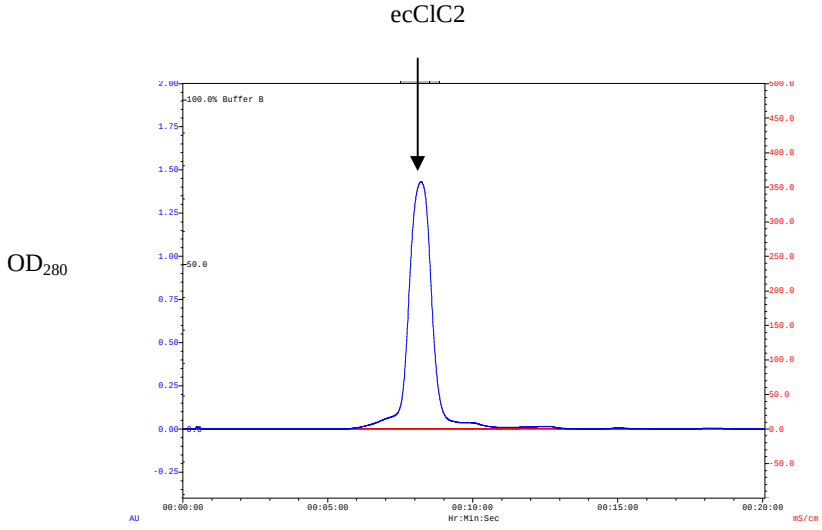

Fig. 3.3 Chromatogram from size exclusion column SEC 250. The protein was run with buffer V containing DM. ecClC2 elutes from the column as a dimer as compared to molecular weight standards run on the column (Figure 3.4)

Size exclusion chromatography is based on separation by size. The relative size of the protein can be extrapolated from the retention time of the protein. Molecular weight standards were run on the SEC 250 column at the same flow rate (Fig. 3.4). The retention time of ecClC2 was about eight minutes. Comparing this time to the standards, it is between IgG (150kDa) and ovalbumin (44kDa) and is much closer to IgG. This gives an estimate of the molecular weight of the species of just under 150kDa. This is larger than both ecClC2 monomer (50kDa) and dimer (100kDa). The extra size is explained by the detergent micelle surrounding the protein that adds a considerable amount of weight and size to the species.

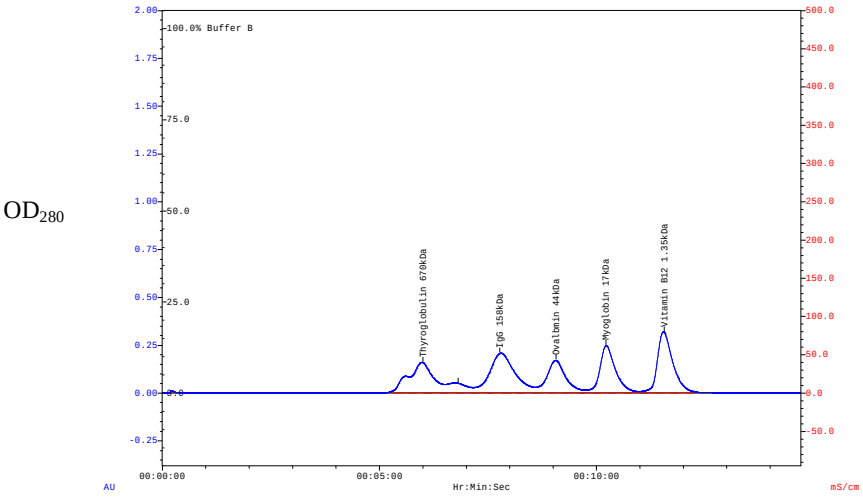

Fig. 3.4. Chromatogram of molecular weight standards run on the SEC 250 column. The molecular weight and name of the components is marked above the peak that corresponds to it.

The pooled fractions from the affinity column run as a single peak with small shoulders on either side of the main peak. Only the main peak was collected for further experiments. The elution profile of ecClC2 on the size exclusion column varied depending on the detergent in which it was solubilized. The elution profile of ecClC2 where the detergent had been exchanged for LDAO on the cobalt affinity column contains a large hump to the left of the main peak (Figure 3.5) that was aggregated protein, as deduced from SDS-PAGE analysis (Figure 3.5). A sample was taken from the peak fraction for SDS-PAGE analysis.

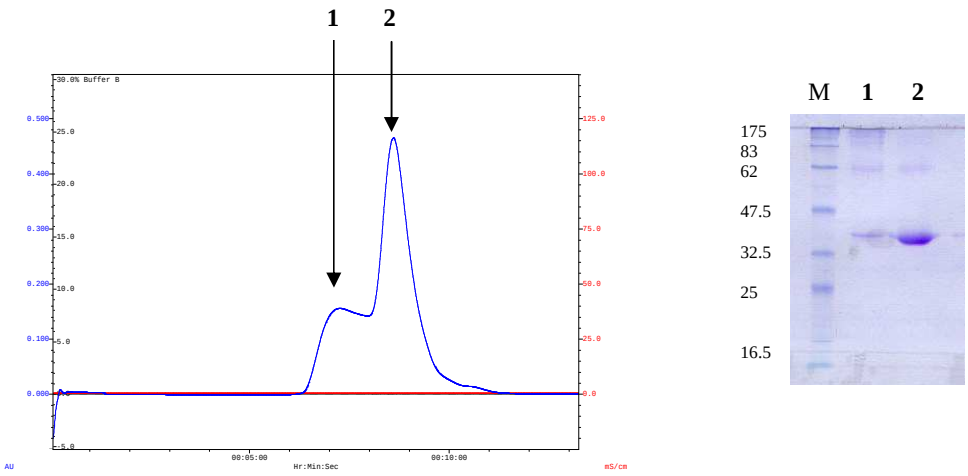

Fig 3.5 Chromatogram from SEC 250 column and 12.5% SDS-PAGE showing aggregation of ecClC2 in LDAO. The high molecular weight species (**1**) and the second peak where ecClC2 usually elutes (**2**) were run on a 12.5% SDS-PAGE gel (left). Both peaks appear to be ecClC2; it was therefore assumed that the higher molecular weight species was aggregated protein rather than an impurity. Only peak 2 was collected.

3.1.6 Preparation for crystallisation experiments

After size exclusion chromatography the protein was judged sufficiently pure for crystallisation trials. Purified protein was concentrated to between 5 and 10mg/ml in a centricon® 30 (Millipore). Concentration of the protein also results in concentration of the detergent in the buffer as the micelles formed by the detergent can be quite large. The concentration of the detergent was lowered by further dialysis. Spectra/Por® 10,000Da molecular weight cut off dialysis membrane (Fischer Scientific UK, Ltd.) was rinsed in deionised water and soaked in buffer VI (50mM Tris pH 8.0; 200mM NaBr; 2-3mM LDAO/DM). The concentrated protein was then placed in the tubing, sealed at both ends and placed in 75ml buffer VI. The protein was left to dialyse overnight at room temperature. Once dialysed the protein was removed from the dialysis tubing and centrifuged for 2 minutes at 15,000rpm to pellet insoluble material and precipitated protein. After this the final concentration measured by the Bradford assay or absorbance at 280nm. The final yield was typically 1mg of pure protein per litre of culture.

3.2 Crystallisation trials

3.2.1 Introduction

Crystallisation of proteins can only be achieved with highly pure and homogenous samples of protein. Three-dimensional protein crystals are usually grown by forming a super-saturated solution and causing precipitation sufficiently slowly, and in such a manner that ordered arrays of the protein are formed. Addition of reagents, such as salts or polyethylene glycols (PEGs), that 'compete' for the water in the protein solution will bring the protein out of solution. Changing the pH of the solution, the addition of a number of organic compounds or changing the temperature can alter the way the protein molecules interact with each other leading to crystallisation. As well as the addition of these additives, the protein solution is usually allowed to slowly increase in concentration, this is accomplished by vapour diffusion. All the crystals described in this chapter were grown using the sitting drop vapour diffusion method (Fig. 3.6). In this method, equal volumes of protein solution and precipitant are mixed in a bridge suspended over a well of precipitant. The system is then sealed to allow the two solutions to equilibrate by vapour diffusion thereby increasing the concentration of the protein in a controlled manner.

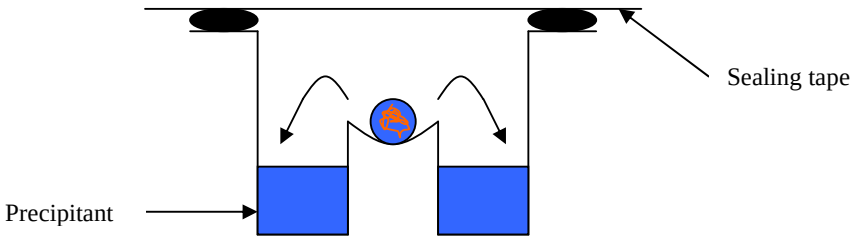

Fig. 3.6 Cross section through a sitting drop vapour diffusion crystallisation chamber. Precipitant (blue) is mixed with protein solution (red) and placed on the bridge in the well. The drop will equilibrate with the precipitant in the well as water diffuses from the drop to the well solution (black arrows).

3.2.2 Sparse matrix screening

In order to find initial crystallisation conditions the protein was screened using various commercially available screening kits. These kits contain reagents that cover a large range of precipitants, pHs and organic compounds. The solutions were pipetted into the reservoirs of 24 well sitting drop crystallisation trays (Charles Supper, Co) in 300µl aliquots. A 2µl drop of ecClC2 (5–10mg/ml) was then placed in the well of each chamber; to these drops 2µl of precipitant from the reservoir was added without further mixing. Each tray was sealed with Crystal Clear Tape (Manco, Inc) and placed in an incubator at 21°C. The protein was initially screened in DM; this produced a few crystals that proved to be of poor quality. Screens were then carried out with LDAO as the detergent. The matrices used were Structure Screen I and II (Molecular Dimensions, Ltd.), Wizard I and II (Emerald Biostructures) and Cryo I and II (Emerald Biostructures). These screens produced crystals in a few conditions (Figure 3.7a and 3.7b and Table 3.2) that appeared overnight.

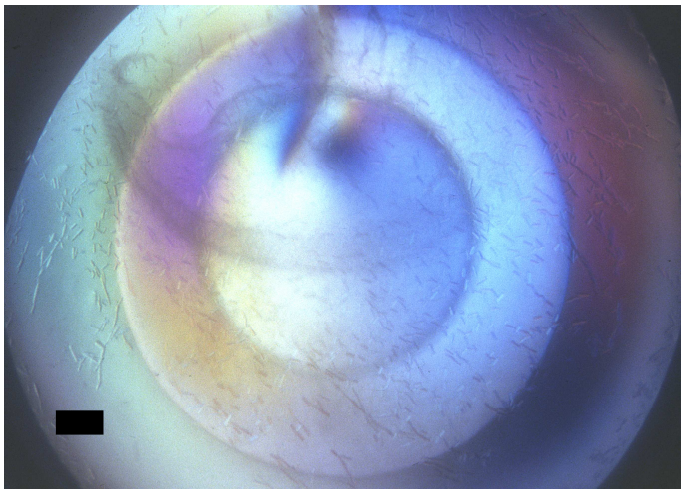

Fig. 3.7a Small rectangular crystals of ecClC2 grown from 0.1M CHES pH9.5 and 30% PEG 3000 (condition number 41 from Wizard I screen) in LDAO; crystals appeared overnight. The bar represents 140µm. A close up of the crystals is shown in Figure 3.7b.

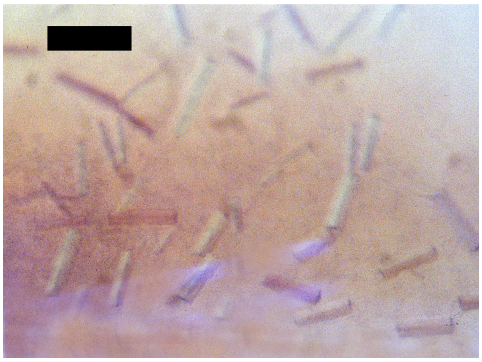

Fig. 3.7b Close up of the crystals shown in Fig. 3.7a. Sharp edges can be seen. The bar represents 100μm.

Screen reagent No	Buffer	Precipitant	Additive
Wizard I # 10	0.1M Tris pH 7	20% PEG 2000MME	None
Wizard I # 27	0.1M CAPS pH10.5	1.2M NaH_2PO_4 0.8M K_2HPO_4	0.2M $LiSO_4$
Wizard I # 41	0.1M CHES pH 9.5	30% PEG 3000	None
Structure Screen I # 31	0.1M HEPES pH 7.5	20% PEG 4000	10% 2-propanol
Structure Screen I # 38	0.1M Tris pH 8.5	8% PEG 8000	None

Table 3.2 Conditions from the sparse matrix screens in which crystals of ecClC2 were grown.

3.2.3 Initial optimisation of conditions

The crystals found in the sparse matrices were too small (less than 20μm in any dimension) and of insufficient quality for X-ray diffraction studies. Efforts to improve crystal quality were informed by diffraction tests on any promising crystals. New solutions were produced that varied the conditions in the matrices such as pH and amount of precipitant. Two strategies were employed: First screens were made

that covered conditions very similar to those in Table 3.2 to try to reproduce the crystals obtained in the initial screen and possibly improve on them. Secondly, broader screens were made up that covered a much larger range of precipitants and pHs. The screens are shown in Tables 3.3, 3.4 and 3.5.

Screen	Precipitant	pH	Additive
PEG 4000 vs pH	16-26% PEG 4000	0.1M HEPES pH 7-8.2	10% 2-propanol (v/v)
PEG 4000 vs 2-propanol	16-26% PEG 4000	0.1M HEPES pH 7.5	5-20% 2-propanol (v/v)
PEG 2000 MME vs pH	16-26% PEG 2000 MME	0.1M Tris pH 6-7.5	None
PEG 3000 vs pH	24-34% PEG 3000	0.1M CHES pH 8.5-10	None

Table 3.3 Screens closely covering the conditions found in the sparse matrices shown in Table 3.2. Precipitant was varied in steps of 2% across 6 wells horizontally; pH and additives were varied across 4 wells vertically.

All screen solutions were made (10ml for each condition) in the following manner:

1. Stocks were prepared of buffer solutions (1M), PEGs (40-60% w/v) and salts, and sterile filtered.
2. The appropriate volume (measured by weight) of PEG stock solution was put into a 15ml tube.
3. 1ml of buffer stock solution was added to the tube.
4. The appropriate amount of salt or additive was added.
5. The solution was made up to 9ml with sterile filtered ddH_2O.
6. Solutions were brought to within 0.01 pH units of the desired pH with HCl or NaOH, and then made up to 10ml.

Screen solutions were stored at 4°C.

Crystallisation experiments were conducted with ecClC2 in LDAO and the screens outlined in table 3.3 in the same manner described in Section 3.2.2. The PEG 4000 screens gave poor results; however the PEG 3000 and 2000 MME screens produced crystals similar to those grown previously and some larger crystals with sharper edges and different morphology (Fig. 3.8).

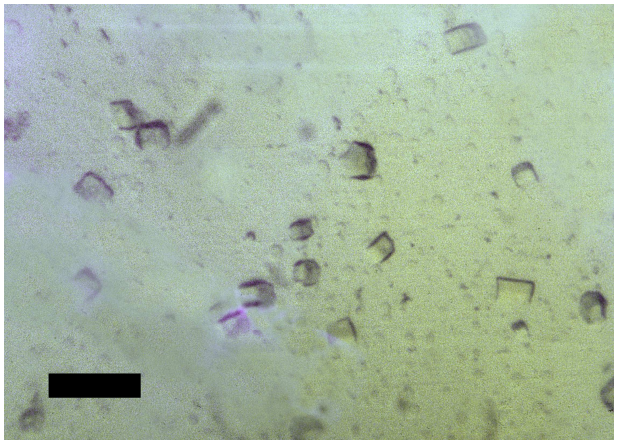

Fig. 3.8 Crystals of ecClC2 grown from 32% PEG 3000 0.1M CHES pH 8.5; crystals usually appeared after 48 hours. The bar represents 60µm.

3.2.4 Optimisation of crystallisation conditions

After the results of the crystallisation trials ecClC2 was put into a much broader matrix that screened mid-range PEGs against pH and salts (Table 3.4 and 3.5). This matrix was prepared as before.

Buffer and pH	PEG					
	20%	25%	30%	35%	40%	45%
0.1M Na acetate pH 5	PEG 1450, 2000, 2000 MME and 2000DME Without salt and with NaBr, $LiSO_4$, Ammonium formate and Ammonium sulphate					
0.1M Na cacodylate pH 6						
0.1M HEPES pH 7						
0.1M Tris pH 8						

Table 3.4 Broad matrix to test for crystallisation conditions of ecClC2.

Buffer and pH	PEG					
	10%	15%	20%	25%	30%	35%
0.1M Na acetate pH 5	PEG 3350, 4000 and 5000 MME Without salt and with NaBr, $LiSO_4$, Ammonium formate and Ammonium sulphate					
0.1M Na cacodylate pH 6						
0.1M HEPES pH 7						
0.1M Tris pH 8						

Table 3.5 Broad matrix to test for crystallisation conditions of ecClC2. Percentages of the PEGs are lower due to the higher molecular weights.

Crystals from this screen were found between pH 6 and 7 around the 20% PEG well. The best crystals were found in 20% PEG 2000 DME at a pH of 7 without any salt (Fig. 3.9). None of the conditions containing salt yielded crystals.

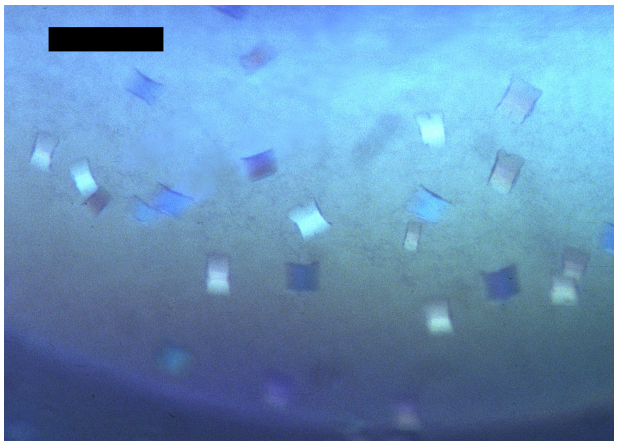

Fig. 3.9 Crystals of ecClC2 grown from 20% PEG 2000 DME 0.1M HEPES pH 7.0, crystals appeared after three to four days. The bar represents 200µm.

These crystals provided a set of crystallisation conditions to make a more focused screen. In the more focused screen, the mid range PEGs were screened over much smaller steps in percentage and between pH 6 and 8 in eight steps (Table 3.6). These screens yielded larger crystals of better quality.

Buffer and pH	PEG					
	16%	18%	20%	22%	24%	26%
0.1M Bis/Tris pH 6.0	PEG 1450, 2000, 2000 MME, 2000DME, Jeffamine ED2001®, 3350, 4000 and 2000 MME : 5000 MME 1:1 mix.					
0.1M Bis/Tris pH 6.25						
0.1M Bis/Tris pH 6.5						
0.1M Bis/Tris pH 6.75						
0.1M Tris pH 7.0						
0.1M Tris pH 7.3						
0.1M Tris pH 7.6						
0.1M Tris pH 8.0						

Table 3.6 Conditions of mid-range PEG focused screen.

Good crystals, measuring approximately 100μm in the largest dimension, grew after 2 to 5 weeks from PEG 2000 MME, 2000 DME (Fig. 3.10) and Jeffamine ED2001®† in the pH 6-6.75 range. The Jeffamine ED2001 screen produced the best crystals after 4 to 5 weeks (Fig.3.11).

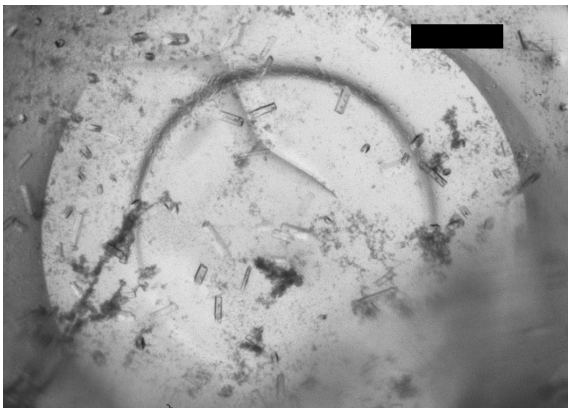

Fig. 3.10 Crystals of ecClC2 grown from 24% PEG 2000 DME 0.1M Bis/Tris pH 6.0. The crystals appeared after two weeks. The bar represents 300μm.

† O,O'-Bis(2-aminopropyl)polyethylene glycol 1900. Crystals initially grown in PEG 4000 have been shown to improve in quality when the precipitant is changed to Jeffamine ED 4000 (Lloyd *et al.* 1994).

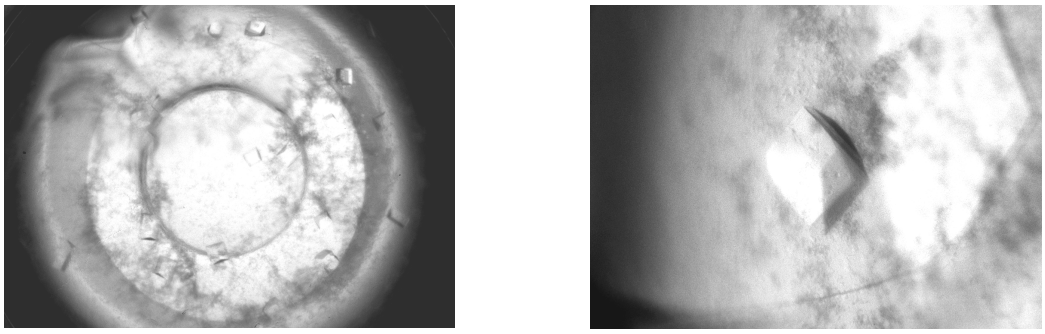

Fig. 3.11 Crystals of ecClC2 grown from 26% Jeffamine ED2001® 0.1M Bis/Tris pH 6.25. The crystals are'cubic' in their morphology and the largest are approximately 100µm x 100µm x 50µm.

As good crystallisation conditions had been established, an additive was screened against the PEG 2000 DME screen. This additive was heptane-1,2,3-triol, a small amphiphilic molecule that is thought to 'shrink' the detergent micelle around a protein thereby producing more ordered crystals (Timmins *et al.* 1991) (Ostermeier and Michel 1997). This additive has been used in the crystallisation of other membrane proteins, with LDAO and other detergents, with success (Deisenhofer *et al.* 1995) (Palczewski *et al.* 2000). Heptane-1,2,3-triol was added to the purified protein before it was placed into the PEG 2000 DME screen, at a concentration of 3% (w/v). Crystals appeared after 2 weeks and showed a slightly different morphology from the previous crystals formed in this screen (Fig. 3.12).

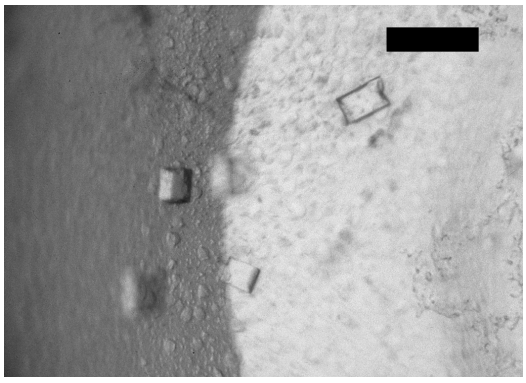

Fig. 3.12 Crystals of ecClC2 grown from 24% PEG 2000 DME 0.1M Bis/Tris pH 6.0 and 3% Heptane-1,2,3-triol. The bar represents 100µm.

3.3 X-ray diffraction from ecClC2 crystals

Crystals were tested for their ability to diffract X-rays as they were produced and this directed the screening of conditions. Crystals were tested in the X-ray generators in the laboratory as well as at synchrotron radiation sources. The results of these experiments are described in this section.

3.3.1 Data collection methods

Once crystals have grown they must be removed from the drop in order to place them in an X-ray beam. Protein crystals are also subject to damage by X-ray radiation therefore data collection is usually performed at 100K. This section describes the methods employed in mounting crystals and protecting them from the X-ray damage and low temperatures.

3.3.1.1 Cryoprotection of crystals

Freezing protein crystals to 100K reduces the amount of damage caused by free radical formation induced by the incident X-rays. Radiation damage in protein crystals can seriously compromise the quality of the data collected (Garman 1999). However, the freezing process itself can damage the crystal by the formation of ordered ice. The ice disrupts the crystal order and diffracts X-rays, thereby interfering with the data. The formation of ice is prevented in two ways: First, the crystal must be frozen extremely quickly to reduce the time available for ordered ice to form. Secondly, the crystallisation mother liquor can be a cryoprotectant or the crystal can be transferred to a solution containing solutions known to cryoprotect (Garman and Schneider 1997). Cryoprotection changes the freezing point and kinetics of the mother liquor; this increases the time taken for ice to form allowing freezing to occur without ice formation. The latter strategy is not optimal where membrane protein crystals are concerned, as it involves transferring the crystal from the mother liquor to another solution. The new solution must also contain detergent, which must be at exactly one times the CMC; too high and the crystal dissolves, too low and the crystal is destroyed. As the CMC of detergents is dependent on the concentration of salt, PEGs, and other components it difficult to add the correct concentration of detergent.

Before crystals were frozen, crystallisation solutions were tested for ice formation by freezing a small droplet in a loop to 100K and looking for diffraction caused by ice. It was found that for the mid-range PEG screens (see Table 3.6), solutions greater that 22% PEG were cryoprotected. Addition of 5% PEG 400 to solutions below this concentration should protect crystals. As the better crystals usually formed above a PEG concentration of 22%, the crystals could be mounted or flash frozen directly from the crystallisation tray. This circumvented the need to transfer crystals to another solution.

3.3.1.2 Crystal mounting

Crystals were mounted in Easyview™ cryoloops (Molecular Dimensions, Ltd), these are rayon or nylon loops with a diameter varying from 0.05 to 0.4mm. The loop is mounted in a nickel 'top hat' that can be placed on the magnetic head of a goniometer (this enables the crystal to be centred on an X-ray beam). Single crystals were scooped out of the drops in the loops surrounded by a small amount of mother liquor. Once the crystal was trapped in the loop it was flash frozen in liquid nitrogen or a stream of dry nitrogen gas at 100K.

3.3.2 'In-house' X-ray diffraction

The crystals produced from the sparse matrix screen (Section 3.2.2, Fig. 3.7) were too small for diffraction experiments, however the crystals produced from the PEG 3000 screen (Table 3.3, Fig.3.8) were of sufficient size to test. Testing of crystal was performed with Cu Kα radiation from a Rigaku rotating anode X-ray generator, diffraction was detected on a Mar-Research 345mm imaging plate area detector. Single crystals were mounted as described in Section 3.3.1.2 and flash frozen in a 100K dry nitrogen gas stream from a Cryostream (Oxford Cryosystems). Crystals were exposed for 30 minutes with an oscillation angle of 1°. Diffraction was observed to a resolution of approximately 20Å.

3.3.3 Synchrotron radiation

Due to the small size and weak diffracting nature of the crystals, synchrotron radiation was required to produce useful data. The crystals grown from PEG 3000 (Section 3.2.3) were taken to the Synchrotron Radiation Source (SRS), Daresbury and mounted on beamline 14.1. Single images were taken only as a test to see if the crystals would diffract further in the more intense beam produced by the synchrotron. The crystals diffracted to approximately 8Å. Following this result, further crystallisation screens were produced to search for better diffracting crystals (Section 3.2.4).

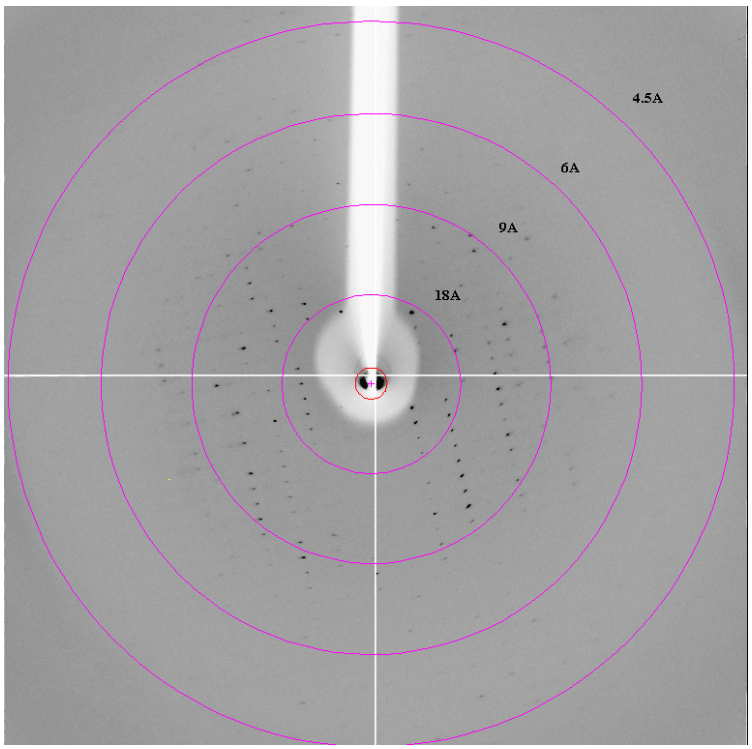

Fig 3.13 Diffraction pattern from a crystal of ecClC2 grown from 24% PEG2000 DME 0.1M Bis/Tris pH 6.0. The image was taken on beamline ID29 at the European Synchrotron Radiation Facility (ESRF) on an ADSC detector (Area Detector Systems Corporation). The resolution is marked on the pattern. Weak diffraction is observed to a resolution of 6Å in one direction.

The crystals obtained in PEG 2000 MME and DME (Table 3.4, Fig. 3.9) were improved on in more focused screens (Table 3.6). Crystals from these screens were

taken to beamline ID29 at the European Synchrotron Radiation Facility (ESRF), Grenoble, France. Crystals were screened by taking a single image at $\phi = 0°$ with an exposure time of 30 seconds and a second at $\phi = 90°$ to look for good diffraction. Initially crystals grown from PEG 2000 MME and DME showed diffraction to approximately 6 Å (Fig. 3.13). Crystals grown in PEG 2000 DME with 3% heptane-1,2,3-triol provided diffraction to a higher resolution. Unfortunately the higher resolution was limited to only one direction (Fig. 3.14).

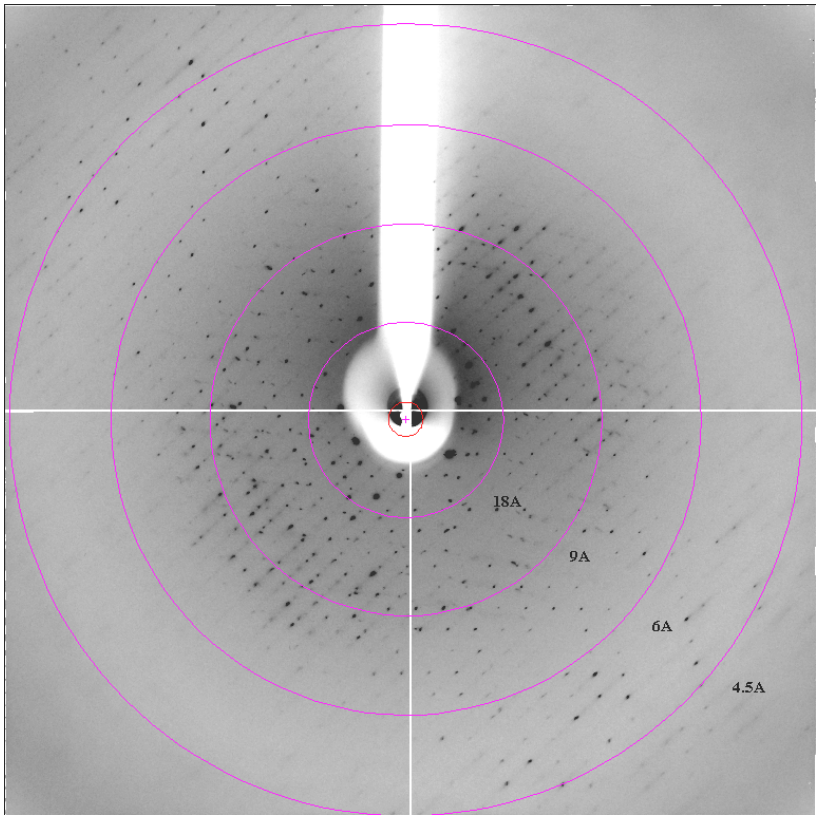

Fig. 3.14 Diffraction pattern from a crystal of ecClC2 grown from 24% PEG 2000 DME 0.1M Bis/Tris pH 6.0 and 3% Heptane-1,2,3-triol. The image was recorded on an ADSC detector (Area Detector Systems Corporation). Spots can be seen beyond 4.5Å but only in one direction. High mosaicity (~3°) is seen and the crystal appears to be twinned. This image was taken from a crystal extracted from the well shown in Figure 3.10.

A data set was collected from the crystal from PEG 2000 DME with 3% heptane-1,2,3-triol (Fig. 3.14). After ten degrees of data had been collected the diffraction limit had reduced dramatically; this may have been due to radiation damage.

Larger crystals were grown in the Jeffamine ED2001® screens (Table 3.6, Fig. 3.11 and 3.16) and were tested on beamline ID14-1 (ESRF). These crystals showed an improvement in the resolution obtained but the mosaicity was still very high (>2°). (Fig. 3.15). A data set was collected from this crystal with little loss of resolution over time.

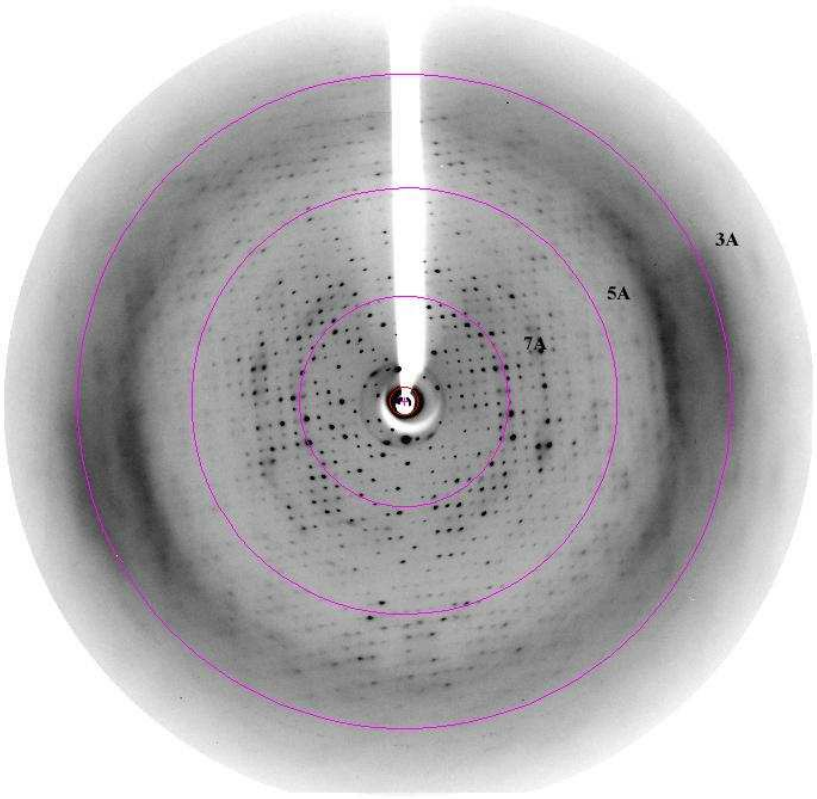

Fig. 3.15 Diffraction pattern from a crystal of ecClC2 grown from 24% Jeffamine ED2001® 0.1M Bis/Tris pH 6.25 (see figure 3.16). The image was taken on a MAR 165mm CCD detector (MAR research) at beamline ID14-1 (ESRF). Diffraction was observed in all directions to approximately 4 Å.

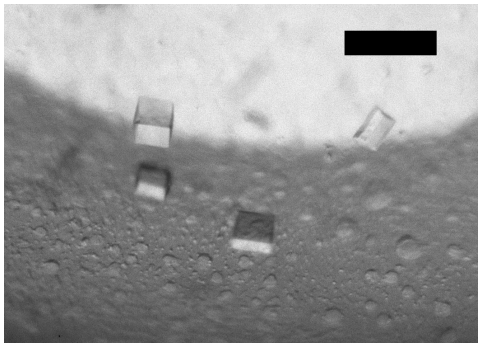

Fig. 3.16 Crystals of ecClC2 that grew from 24% Jeffamine ED2001® 0.1M Bis/Tris pH 6.25 after 5 weeks. The bar represents 100μm. These crystal diffracted to 4 Å (Fig. 3.15).

3.3.4 Data analysis

The data set collected on the crystal grown in Jeffamine ED2001® (Fig. 3.15) was of sufficient quality to be able to begin diffraction image analysis. The data were analysed in the program Mosflm, part of the CCP4 suite of programs (CCP4 1994). Analysis of the data set revealed that the crystal had a primitive orthorhombic space group. The unit cell has the dimensions 97Å x 104Å x 140Å. The number of molecules in the unit cell can be calculated from the unit cell dimensions, the space group and the known properties of the molecule (Matthews 1968). The ratio between molecular weight and unit cell volume is usually between 1.7 and 3.5$Å^3$/Da. Orthorhombic space groups have four repeats, therefore, the calculated ratio for ecClC2 is 3.53$Å^3$/Da for a dimer in the asymmetric unit and 1.76$Å^3$/Da for two dimers in the asymmetric unit. Either of these values could be correct. By calculating the solvent content of the crystal the more likely solution can be found. By dividing the specific volume of ecClC2 (0.755 cm3/g) by the unit cell to molecules ratio multiplied by Avogadro's number, the fractional proportion of protein to solvent is obtained. For a ratio of 1.76$Å^3$/Da the calculated solvent content is 30%, this is very low for a protein crystal. The ratio of 3.53$Å^3$/Da gives a value of 65% solvent, a more realistic value. The most likely number of molecules in the asymmetric unit is,

therefore two monomers, however as the ratios are so close to the upper and lower limits the value is by no means conclusive.

3.4 Conclusions

Crystals of ecClC2 have been obtained that demonstrate diffraction to a sufficiently high resolution that improvement of the crystal quality will allow image analysis to proceed. This makes the determination of the structure feasible. The quality of the diffraction is still not good enough for complete image analysis but there are still experiments that may improve the crystal quality. These experiments and the work that remains to solve the structure are outlined in Chapter 4.

CHAPTER 4:

FURTHER WORK AND CONCLUSION

Chapter 3 described the purification of ecClC2, conditions for its crystallisation and preliminary X-ray diffraction analysis of the crystals. The methods described produces crystals that show reasonable diffraction; although the crystals are not yet of sufficient quality to enable structural analysis. Some methods that may improve the quality of the crystals, and work that remains in order to solve the structure of ecClC2, are outlined in this chapter.

4.1 Optimisation of Crystallisation conditions

4.1.1 Initial conditions

Although conditions that produce good crystals have been found (as described in chapter 3), there is still potential to alter these conditions to improve crystal quality. The range over which the concentration of Jeffamine ED2001® and pH are screened can be narrowed to find the optimum concentrations for crystal formation.

4.1.2 Additives

A large range of additives can be screened against the known crystallisation conditions. Additives can vary from salts to small organic compounds. Heptane-1,2,3-triol has not been screened with the crystals grown in Jeffamine. This additive improved the quality of diffraction obtained from crystals grown in PEG 2000 DME (see section 3.2.4 in chapter 3). Other additives that are thought to shrink the detergent micelle surrounding a protein are benzamidine and dioxane. These additives have been used successfully in the crystallisation of membrane proteins (Papiz *et al.* 1989) (Buchanan *et al.* 1993). Inhibitors of ClC channels may yield better diffracting crystals by reducing any flexibility in the protein. Several inhibitors of ClC channels exist that inhibit most of the eukaryotic ClC family. In principle these inhibitors should also be effective on ecClC2 . Chlorotoxin from the scorpion *Leiurus quinquestriatus* (DeBin *et al.* 1993) is the most potent ClC channel blocker

known, but it is a bulky peptide which may interfere with crystallisation. Other molecules that contain a negative thiocyanate group attached to phenol groups such as DIDS (4,4'-diisothiocyanostilbene-2,2'-disulphonic acid) and NPPB (5-nitro-2-(3-phenylpropylamino) benzoic acid) have been found to be very effective in reducing chloride currents in eukaryotic ClC channels (Bettendorff *et al.* 1995) (Alton and Williams 1992). Zinc ions have also been found to reduce chloride currents in ClC-1 (Kurz *et al.* 1997) (Kurz *et al.* 1999). Screening these inhibitors may produce less flexible ecClC2 molecules and result in more favourable intermolecular contacts within the crystal, and therefore better diffracting crystals.

4.1.3 Detergents

The crystals of ecClC2 were grown in the presence of the detergent lauryldimethylamine N-oxide (LDAO). The detergent used has a large effect on the quality of crystals as it surrounds the protein. Micelle shrinking additives can have a profound effect as can the head group and tail length of the detergent (Ostermeier and Michel 1997). Trials in which the detergent's chain length is changed may yield better quality crystals. Detergents which have the same head group as LDAO but chain lengths varying from 10 (Decyldimethylamine N-oxide, DDAO) to 13 (Tridecyl dimethylamine N-oxide, TDAO) are commercially available. Detergents with different head groups may have to be tested to obtain the best quality crystals.

4.1.4 Lipidic cubic phase crystallisation

Changing the method of crystallisation may affect the crystal type and quality. One method that has already been tried with ecClC2 during the course of the project, is crystallisation within a lipidic cubic phase (these experiments are not described in this thesis). This method was used to crystallise bacteriorhodopsin and has been shown to produce good crystals of other membrane proteins (Landau and Rosenbusch 1996) (Chiu *et al.* 2000). The crystals formed in a cubic phase are type I crystals as opposed to type II formed in the sitting drop method. Type I crystals are layers of two-dimensional crystals that form ordered three-dimensional crystals; the crystals contain no detergent. Type II crystals form contacts only with the polar surface of the protein and detergent is present in the crystal; these crystals tend to be less ordered than type I crystals.

When a solution of protein solubilised in detergent is mixed with monoolein the cubic phase forms spontaneously. The cubic phase forms a continuous bilayer of the lipid in three-dimensional 'cubes'. When the two solutions are mixed, the protein abandons the detergent micelle and enters the lipid bilayer, which more accurately represents a natural environment (Landau and Rosenbusch 1996). In order to initiate crystallisation, a precipitant, usually a salt, is added to the cubic phase. The salt 'competes' for the water in the cubic phase destabilising it. This causes the protein to come out of solution and begin crystallisation (Caffrey 2000). Several trials, screening ecClC2 in a lipidic cubic phase against various precipitants, have been set up. Although the trials have not been successful, this method may eventually yield crystals of better quality than those produced by the sitting drop vapour diffusion method.

4.1.5 Conclusions

Conditions have been found that produce crystals of ecClC2 that show promising diffraction. These conditions require manipulation until crystals are obtained that will diffract X-rays to a higher resolution and produce a diffraction pattern of better quality than those already obtained (see chapter 3, section 3.3.3). There are still many experiments to be tried to optimise the crystals, and in principle it should be possible to grow better crystals.

4.2 Determination of the structure

Once the crystals have been optimised and a complete native data set has been collected the maximum resolution, data to obtain the phases will have to be collected. The diffraction patterns obtained are measures of the intensity of the diffracted X-rays but not on the relative phases of the X-rays; both are required to calculate the electron density of the protein's atoms. This lack of phase information is generally referred to as the 'phase problem' in macromolecular structure elucidation. This section briefly outlines the phase problem and some methods of solving it.

4.2.1 The phase problem

Diffraction patterns are the result of interference between X-rays that are scattered by electrons in an ordered crystal. The spots found in a diffraction pattern are the result of constructive interference between diffracted X-rays. The position of the spots is determined by the crystal lattice and the molecular structure of the crystalline material. The intensity of the spots is determined by the crystal structure and the atomic structure of the crystalline material. The intensity is proportional to the amplitude squared of the diffracted X-rays. The spacing of the spots will provide structural information on the crystal such as space group and the dimensions of the unit cell. However, solving the atomic structure of the substance forming the crystal requires both the magnitude and relative phases of the X-rays (Bragg and Bragg 1915). X-rays which are diffracted by the electron density in the crystal differ in their magnitude and phase (the relative position of the waveform with respect to an origin, (see Figure 4.1) from X-rays which are not scattered). These differences are caused by the diffracting material and knowledge of them is essential to obtain the structure of the crystalline material; as the inverse Fourier transform of the phase and magnitude corresponds to the electron density within the unit cell (Titchmarsh 1937). As the phases cannot be directly measured, other methods are required to obtain the phase values. One of these methods, anomalous scattering, is outlined in the next section.

4.2.2 Anomalous scattering

All atoms absorb X-rays to a certain extent; the likelihood of an atom absorbing X-rays increases with the atomic number due to the large number of electrons it possesses. The level at which a certain atom absorbs X-rays increases sharply when the wavelength of the incident X-rays is similar to the natural resonance levels of the electrons in an atom. This wavelength is referred to as the absorption edge of a particular atom and is unique to each atom. If a crystal contains heavy atoms and is irradiated with X-rays of a wavelength close to that of the absorption edge, the magnitude and phase of the scattered X-rays will be different to those of the native data. This change is called anomalous scattering. By comparing the values of the magnitudes, two possible values of the phases can be calculated by a method known as the Harker construction (Harker 1959).

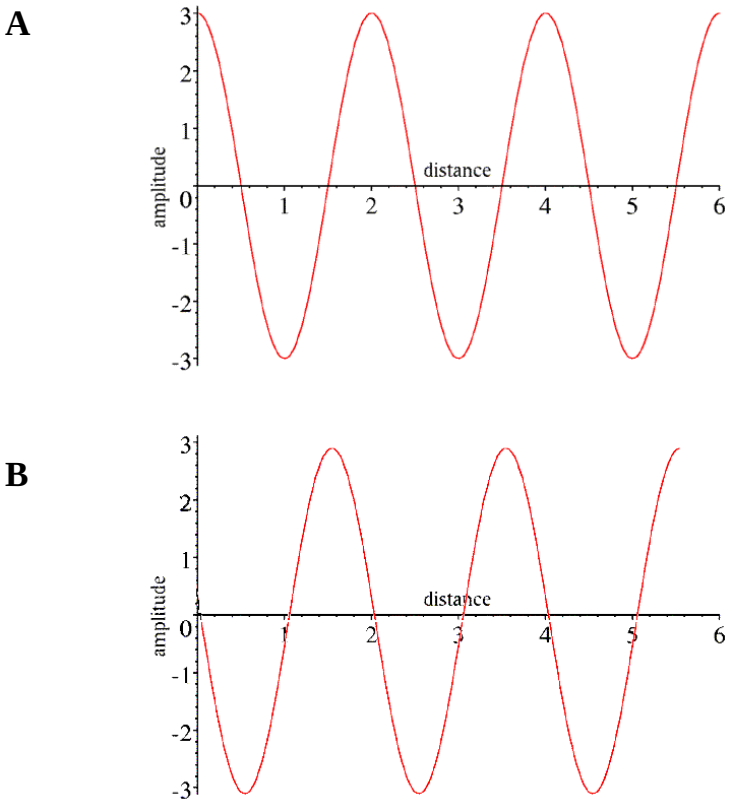

Fig. 4.1 Two simple waves that are out of phase with respect to each other. Wave A has maximum amplitude at a distance of zero whereas wave B has maximum amplitude at a distance of 1.5; therefore, the phase difference between the waves is 1.5. The units are arbitrary. Adapted from (Bloomer *et al.* 1999).

By collecting data sets from crystals containing heavy atoms at several wavelengths near to the absorption edge of that heavy atom, different changes in magnitude will be recorded for the heavy atom. From these data, the actual values of the phases can be calculated. This method is called Multiple-wavelength Anomalous Dispersion (MAD) (Hendrickson 1991). This technique requires synchrotron radiation as a variety of wavelengths are required and some synchrotron beamlines can be tuned, whereas in-house sources cannot.

4.2.3 Introducing heavy atoms into ecClC2 crystals

There are many methods by which heavy atoms can be introduced into a protein crystal. One method is to replace natural amino acids with those containing a heavy atom. One such amino acid is seleno-methionine; this is an equivalent of methionine where the sulphur is replaced by a selenium atom. Introducing this molecule involves producing the protein in medium which is deficient in methionine but is supplemented with seleno-methionine. In principle, the seleno-methionine is incorporated into the protein and crystals grown from the preparation will contain selenium. Another method is to introduce cysteine residues into the protein by site directed mutagenesis. The free sulphydryl groups of cysteines react strongly with some heavy metals such as mercury. By soaking crystals in a mother liquor solution containing a heavy metal salt, the heavy metal ions will diffuse into the crystal through the large solvent channels and bind to the sulphydryl groups. This method has disadvantages when applied to ecClC2. As described in section 3.3.1.2 of Chapter 3, the solution in which a membrane protein crystal is to be soaked must contain detergent at exactly the value of the CMC; this is a very difficult value to measure. Bromine has been used as the heavy atom in MAD experiments to obtain the phases and solve the structures of unknown proteins (Ho *et al.* 2000) (Hoover *et al.* 2000) (Devedjiev *et al.* 2000) and has been demonstrated as a useful tool by re-solving many known structures (Dauter *et al.* 2000). The crystals are soaked in a solution containing a high concentration of bromide ions in the hope that the ions will bind to the protein through van der Waals forces or hydrogen bonding with amino groups (Dauter *et al.* 2001). The purification and crystallisation of ecClC2 was performed in the presence of 200mM sodium bromide (Chapter 3, sections 3.1 and 3.2). While this concentration may not be high enough to have enough bromide ions occupying the same sites by van der Waals forces or hydrogen bonds (Dauter, Li et al. 2001) the ions may be bound to sites in the ion conduction pathway (see Chapter 1, Section 1.2.2).

4.3 Conclusions

This thesis has documented the development of procedures required to ultimately obtain structural information on the *E.coli* chloride channel ecClC2. This has involved the cloning of the gene of interest, the design of an expression system and the growth of good quality crystals. The methods are now in place to enable further experimentation to obtain, in principle, a native data set of sufficient quality and resolution of below 4Å so that structure determination can proceed. Once this has been achieved, phase information will be collected using one of the methods outlined in section 4.2.2. Solving the structure of this channel should provide a detailed explanation of chloride conductance and channel architecture. This will contribute enormously to the understanding of this important family of channels. ClC channels have wide ranging physiological roles and there are many diseases where malfunctioning ClC chloride channels are known, or suspected to be causative. Further characterisation of these diseases should be aided by the structure of this ClC homologue. Questions that may be addressed by the structure include: the number of transmembrane helices, why certain residues are important in chloride conduction and what might be the mechanism of channel gating. Mechanisms have been proposed for some of these unresolved questions with reference to results from electrophysiological and other experiments; however, only direct structural information can provide definitive answers to these questions. It will be fascinating to see the structure and mechanism of this channel solved, let it be pursued.

Appendix:

Biochemical Methods

A.1. Agarose Gel Electrophoresis

Agarose gels were prepared by adding agarose MP (Roche Diagnostics, Ltd.) to TAE buffer (4mM Tris-acetate, 1mM EDTA) to form an appropriate percentage (w/v) solution (e.g. 0.7g agarose in 70ml TAE buffer for a 1% gel). The mixture was then heated in a microwave oven to dissolve the agarose. Once the agarose had dissolved, the solution was poured into a gel caster system (Bio-Rad Laboratories, Ltd) to form a slab gel with wells. DNA samples were prepared by adding 1-5µl of sample to 1µl 6x loading dye (0.25% bromophenol blue, 0.25% xylene cyanol FF, 30% glycerol) and making the volume up to 6µl with TAE buffer. Gels were run with a constant voltage of 120V in a Wide Mini-Sub Cell GT (Bio-Rad Laboratories, Ltd) for 30 minutes or until the dye front had reached the end of the gel. DNA was visualised by staining the gel in a 0.001% ethidium bromide solution for 30 minutes and fluorescing under UV light. The exact sizes and amount of the DNA molecular weight markers, used when running all agarose gels, is shown in figure A.1.

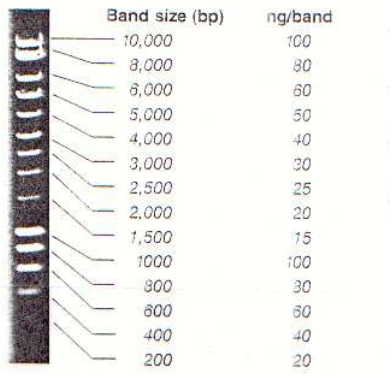

Fig. A.1 Composition of the DNA molecular weight markers shown in the gels. The figure shows 5µl of the DNA molecular weight marker run on a 1% agarose gel stained with ethidium bromide.

A.2. Sodium Dodecyl Sulphate Polyacrylamide Gel Electrophoresis (SDS-PAGE)

SDS-PAGE was performed according to Laemmli conditions (Laemmli 1970) with some modifications that are outlined in this section. All samples were run on 12% gels under non-denaturing conditions. The composition of the stacking and resolving gels is shown in table A.1. Gels were cast and run in the Mini-PROTEAN 3 system (Bio-Rad Laboratories, Ltd). Samples (1-16µl) were mixed with 5µl 4x loading buffer (100mM Tris-HCl, 4% SDS, 0.2% bromophenol blue, 20% glycerol) and made up to 20µl with running buffer. Broad range prestained protein markers (New England Biolabs, U.K, Ltd.) 10µl, were run as a reference in all gels. Gels were run at a constant voltage of 200V for approximately 60 minutes or until the dye front had reached the end of the gel. Protein was visualised by using the staining buffer (40% methanol, 10% acetic acid, 0.1% Coomassie blue R-250) and then destained by several washes in destain buffer (40% methanol, 10% acetic acid).

Stock Solution	Stacking Gel (4%)	Separating Gel (12%)
ddH_2O	6.43ml	4.35ml
0.5M Tris-HCl pH 6.8	2.5ml	0ml
1.5M Tris-HCl pH 8.8	0ml	2.5ml
10% (w/v) SDS	100µl	100µl
Acrylamide/Bis-acrylamide 40% solution	1ml	3ml
10% ammonium persulphate	50µl	50µl
TEMED	10µl	5µl
Total volume	10ml	10ml

Table A.1. Composition of gels used in SDS-PAGE.

A.3. Composition and preparation of bacterial growth media

A.3.1 Luria-Bertani Medium

Luria-Bertani medium (LB) was prepared by adding the following components to a 4l baffled flask. LB Medium Components (per litre): 10g bacto-tryptone, 5g yeast extract and 10g sodium chloride. The medium was sterilised by autoclaving at 121°C, 15lb/sq. in. for 20 minutes.

A.3.2 Terrific Broth

Terrific Broth (TB) was prepared as in section A.3.1 with the following components: 12g bacto-tryptone, 24g yeast extract and 4ml glycerol per litre. The components were added to a 4l flask and 900ml ddH_2O was added and the medium was autoclaved. Once the medium had cooled 100ml of 10x sterile filtered phosphate buffer (0.17M KH_2PO_4, 0.72M K_2HPO_4) was added.

A.3.3 Super Broth

Super Broth (SB) was prepared as in section A.3.1 with the following components: 32g bacto-tryptone, 20g yeast extract and 5g sodium chloride.

A.4. Transformations

DNA manipulation and expression strains of *E.coli* were transformed with plasmid DNA using the heat-shock method. Chemically competent strains of *E.coli* (50µl) were thawed on ice for 5 minutes. Approximately 1µl of plasmid DNA was then added and the cells were incubated on ice for 30 minutes. The cells were then heat-shocked at 42°C for 30 seconds in a water bath. After heat shock the cells were incubated on ice for a further 2 minutes. After incubation on ice, 950µl LB broth was added and the cells were incubated at 37°C in an orbital incubator for 30 minutes. After this recovery period 250µl of the cells were plated out onto LB agar plates containing 50µg/ml kanamycin to select for successful transformants. Plates were incubated overnight at 37°C and inspected for single colonies the following day.

A.5. Preparation of competent cells

Competent *E.coli* strains were prepared in advance of transformations by a modified Hanahan method (Hanahan *et al.* 1991). A 5ml culture of the desired strain was grown in 5ml LB broth overnight at 30°C. 1ml of this culture was then used to inoculate 100ml LB broth. This culture was incubated at 37°C in an orbital incubator. Once the OD_{600} reached 0.5 the cells were immediately transferred to centrifuge tubes pre-chilled to 4°C. Cells were pelleted by centrifugation at 5000rpm at 4°C for 20 minutes in a Beckman Avanti™ J-20 centrifuge. The supernatant was discarded and the cells were resuspended in ice-cold CCMB solution (see Table A.2) and incubated at 4°C for 20 minutes. The cells were then pelleted as before and the supernatant discarded. The cells were then resuspended in 8ml ice-cold CCMB solution. Aliquots of the cells (100µl) were transferred to 1.7ml microfuge tubes and flash frozen in a dry-ice/ethanol bath. Competent cells were stored at -80°C.

CCMB Solution	
Component	Concentration
Calcium chloride	80mM
Manganese chloride	20mM
Magnesium chloride	10mM
Potassium acetate	10mM
Redistilled glycerol	10% (v/v)

Table A.2. Components of CCMB Solution. All chemicals were of the highest grade and solutions were prepared using molecular biology grade water (Sigma).

A.6. Qiagen DNA purification kits

All Qiagen DNA purification kits were used according to manufacturer's instructions.

A.7. Bradford Assay

Protein concentration was estimated by the Bradford assay (Bradford 1976). 400µl ddH_2O was added to 400µl Bradford reagent, mixed and placed in a polystyrene cuvette (Fischer Scientific, Ltd.) and used as a blank. Protein samples were added to an appropriate volume of ddH_2O to make the volume up to 400µl. This solution was then mixed with 400µl Bradford reagent. Protein concentration is directly proportional to the absorbance at 595nm in the presence of Bradford reagent. An Ultrospec 2000 UV/Visible spectrophotometer (Amersham Parmarcia Biotech U.K, Ltd.) was used to measure absorbance. The spectrophotometer was zeroed using the Bradford/water mix and then the absorbance of the sample containing protein was measured. The absorbance was compared to a standard curve that had been plotted using known quantities of Bovine Serum Albumin (BSA). In this way the concentration of a protein sample could be estimated. As the Bradford assay is quite inaccurate and detergents can interfere with the dye, protein concentration was also measured by the absorbance at 280nm. This method is described in section A.8.

A.8. Calculation of concentration from absorbance at 280nm

Measurement of protein concentration by the absorbance at 280nm (OD_{280}) is a non-destructive method. The level to which proteins will absorb UV light at 280nm depends on the number of tryptophan, tyrosine and cysteine residues it contains. This will vary between proteins and each will have an individual molar extinction coefficient. This can be calculated from the number of these residues found in a protein (Gill and von Hippel 1989). Both wild type and recombinant ecClC2 contain the same number of these residues: Tryptophan: 6; tyrosine: 9 and cysteine: 3. The molar extinction coefficient is calculated by multiplying the molar extinction coefficient for each amino acid by the number present in the protein and adding the total.

Amino Acid	Extinction coefficient at 280nm	No. residues in ecClC2	Total	Molar extinction coefficient for ecClC2 at 280nm
Tryptophan	5690 M^{-1} cm^{-1}	6	34140 M^{-1} cm^{-1}	46020 M^{-1} cm^{-1}
Tyrosine	1280 M^{-1} cm^{-1}	9	11520 M^{-1} cm^{-1}	
Cysteine	120 M^{-1} cm^{-1}	3	360 M^{-1} cm^{-1}	

Table A.3. Molar extinction coefficients of the amino acids and calculation of the molar extinction coefficient of ecClC2.

With the molar extinction coefficient calculated the concentration of the protein can be measured from the OD_{280} using the Beer- Lambert law (Fig. A.2). The equation allows the calculation of the molar concentration of the protein from the OD_{280} and molar extinction coefficient.

$$OD_{280} = \varepsilon \times c \times l$$

Fig. A.2 The Beer-Lambert equation where ε is the molar extinction coefficient in M^{-1} cm^{-1}; c is the concentration of the sample in Moles (M) and l is the path length of the cell in cm.

Concentration was measured by placing a sample of the protein in a quartz cuvette with a path length of 1cm and measuring the OD_{280} in an Ultrospec 2000 UV/Visible spectrophotometer (Amersham Parmarcia Biotech U.K, Ltd.) that had been blanked against a cuvette containing buffer only. The molar concentration of the protein was then calculated by dividing the OD_{280} by the molar extinction coefficient (a rearrangement of the above equation).

A.9 Oligonucleotide primers

All primers were purchased from Sigma-Genosys, Ltd. to 0.02μM scale and purified by desalting. Primers arrived as a lyophilised sample. The primers were resuspended in 200μl ddH_2O. The concentration was then calculated by reading the absorbance of the sample at 260nm (OD_{260}). An absorbance of 1unit at 260nm is equal to a concentration of 33μg/ml of single stranded DNA. Once the concentration was known 50μg/ml stocks were made in ddH_2O and stored at -80°C.

References

Adachi, S., S. Uchida, H. Ito, M. Hata, M. Hiroe, F. Marumo and S. Sasaki (1994). "Two isoforms of a chloride channel predominantly expressed in thick ascending limb of Henle's loop and collecting ducts of rat kidney." J Biol Chem **269**(26): 17677-83.

Alberts, B., D. Bray, J. Lewis, M. Raff, K. Roberts and D. Watson (1989). Molecular Biology of the Cell. New York, Garland Publishing, Inc.

Alton, E. W. and A. J. Williams (1992). "Modification of gating of an airway epithelial chloride channel by 5- nitro-2-(3-phenylpropylamino)benzoic acid (NPPB)." J Membr Biol **128**(2): 141-51.

Altschul, S. F., W. Gish, W. Miller, E. W. Myers and D. J. Lipman (1990). "Basic local alignment search tool." J Mol Biol **215**(3): 403-10.

Bateman, A. (1997). "The structure of a domain common to archaebacteria and the homocystinuria disease protein." Trends Biochem Sci **22**(1): 12-3.

Beck, C. L., C. Fahlke and A. L. George, Jr. (1996). "Molecular basis for decreased muscle chloride conductance in the myotonic goat." Proc Natl Acad Sci U S A **93**(20): 11248-52.

Bettendorff, L., I. Margineanu, P. Wins and T. Grisar (1995). "An atypical anion transporter functioning at acid pH in neuroblastoma cells." Biochem Biophys Res Commun **207**(1): 375-81.

Blattner, F. R., G. Plunkett, 3rd, C. A. Bloch, N. T. Perna, V. Burland, M. Riley, J. Collado-Vides, J. D. Glasner, C. K. Rode, G. F. Mayhew, J. Gregor, N. W. Davis, H. A. Kirkpatrick, M. A. Goeden, D. J. Rose, B. Mau and Y. Shao (1997). "The complete genome sequence of Escherichia coli K-12." Science **277**(5331): 1453-74.

Bloomer, A., G. Evans, P. Evans, A. Lesk, A. Leslie, A. McCoy and R. Read (1999). Protein Crystallography Course, Structural Medicine, Department of Haematology, University of Cambridge. **2001**.

Bradford, M. M. (1976). "A rapid and sensitive method for the quantitation of microgram quantities of protein utilizing the principle of protein-dye binding." Anal Biochem **72**: 248-54.

Bragg, W. H. and W. L. Bragg (1915). X-rays and Crystal structure. London, G. Bell and Sons.

Brandt, S. and T. J. Jentsch (1995). "ClC-6 and ClC-7 are two novel broadly expressed members of the CLC chloride channel family." FEBS Lett **377**(1): 15-20.

Buchanan, S. K., G. Fritzsch, U. Ermler and H. Michel (1993). "New crystal form of the photosynthetic reaction centre from Rhodobacter sphaeroides of improved diffraction quality." J Mol Biol **230**(4): 1311-4.

Buyse, G., D. Trouet, T. Voets, L. Missiaen, G. Droogmans, B. Nilius and J. Eggermont (1998). "Evidence for the intracellular location of chloride channel (ClC)-type proteins: co-localization of ClC-6a and ClC-6c with the sarco/endoplasmic-reticulum Ca2+ pump SERCA2b." Biochem J **330**(Pt 2): 1015-21.

Caffrey, M. (2000). "A lipid's eye view of membrane protein crystallization in mesophases." Curr Opin Struct Biol **10**(4): 486-97.

C. C. P. 4. (1994). "The CCP4 suite: Programmes for protein crystallography." Acta Crystallogr D Biol Crystallogr **50**: 760 – 763

Chen, T. Y. and C. Miller (1996). "Nonequilibrium gating and voltage dependence of the ClC-0 Cl- channel." J Gen Physiol **108**(4): 237-50.

Chiu, M. L., P. Nollert, M. C. Loewen, H. Belrhali, E. Pebay-Peyroula, J. P. Rosenbusch and E. M. Landau (2000). "Crystallization in cubo: general applicability to membrane proteins." Acta Crystallogr D Biol Crystallogr **56**(Pt 6): 781-4.

Chou, C. Y., M. R. Shen and S. N. Wu (1995). "Volume-sensitive chloride channels associated with human cervical carcinogenesis." Cancer Res **55**(24): 6077-83.

Claros, M. G. and G. von Heijne (1994). "TopPred II: an improved software for membrane protein structure predictions." Comput Appl Biosci **10**(6): 685-6.

Dauter, Z., M. Dauter and K. R. Rajashankar (2000). "Novel approach to phasing proteins: derivatization by short cryo- soaking with halides." Acta Crystallogr D Biol Crystallogr **56**(Pt 2): 232-7.

Dauter, Z., M. Li and A. Wlodawer (2001). "Practical experience with the use of halides for phasing macromolecular structures: a powerful tool for structural genomics." Acta Crystallogr D Biol Crystallogr **57**(Pt 2): 239-49.

DeBin, J. A., J. E. Maggio and G. R. Strichartz (1993). "Purification and characterization of chlorotoxin, a chloride channel ligand from the venom of the scorpion." Am J Physiol **264**(2 Pt 1): C361-9.

Deisenhofer, J., O. Epp, I. Sinning and H. Michel (1995). "Crystallographic refinement at 2.3 A resolution and refined model of the photosynthetic reaction centre from Rhodopseudomonas viridis." J Mol Biol **246**(3): 429-57.

Devedjiev, Y., Z. Dauter, S. R. Kuznetsov, T. L. Jones and Z. S. Derewenda (2000). "Crystal structure of the human acyl protein thioesterase I from a single X-ray data set to 1.5 A." Structure Fold Des **8**(11): 1137-46.

Doyle, D. A., J. Morais Cabral, R. A. Pfuetzner, A. Kuo, J. M. Gulbis, S. L. Cohen, B. T. Chait and R. MacKinnon (1998). "The structure of the potassium channel: molecular basis of K+ conduction and selectivity." Science **280**(5360): 69-77.

Duan, D., C. Winter, S. Cowley, J. R. Hume and B. Horowitz (1997). "Molecular identification of a volume-regulated chloride channel." Nature **390**(6658): 417-21.

Eggermont, J., G. Buyse, T. Voets, J. Tytgat, H. De Smedt, G. Droogmans and B. Nilius (1997). "Alternative splicing of ClC-6 (a member of the CIC chloride-channel family) transcripts generates three truncated isoforms one of which, ClC-6c, is kidney-specific." Biochem J **325**(Pt 1): 269-76.

Fahlke, C. (2000). "Molecular mechanisms of ion conduction in ClC-type chloride channels: lessons from disease-causing mutations." Kidney Int **57**(3): 780-6.

Fahlke, C. (2001). "Ion permeation and selectivity in ClC-type chloride channels." Am J Physiol Renal Physiol **280**(5): F748-57.

Fahlke, C., R. R. Desai, N. Gillani and A. L. George, Jr. (2001). "Residues lining the inner pore vestibule of human muscle chloride channels." J Biol Chem **276**(3): 1759-65.

Fahlke, C., C. Durr and A. L. George, Jr. (1997a). "Mechanism of ion permeation in skeletal muscle chloride channels." J Gen Physiol **110**(5): 551-64.

Fahlke, C., T. Knittle, C. A. Gurnett, K. P. Campbell and A. L. George, Jr. (1997b). "Subunit stoichiometry of human muscle chloride channels." J Gen Physiol **109**(1): 93-104.

Fahlke, C., T. H. Rhodes, R. R. Desai and A. L. George, Jr. (1998). "Pore stoichiometry of a voltage-gated chloride channel." Nature **394**(6694): 687-90.

Fahlke, C., A. Rosenbohm, N. Mitrovic, A. L. George, Jr. and R. Rudel (1996). "Mechanism of voltage-dependent gating in skeletal muscle chloride channels." Biophys J **71**(2): 695-706.

Fahlke, C., R. Rudel, N. Mitrovic, M. Zhou and A. L. George, Jr. (1995). "An aspartic acid residue important for voltage-dependent gating of human muscle chloride channels." Neuron **15**(2): 463-72.

Fahlke, C., H. T. Yu, C. L. Beck, T. H. Rhodes and A. L. George, Jr. (1997c). "Pore-forming segments in voltage-gated chloride channels." Nature **390**(6659): 529-32.

Fisher, S. E., G. C. Black, S. E. Lloyd, E. Hatchwell, O. Wrong, R. V. Thakker and I. W. Craig (1994). "Isolation and partial characterization of a chloride channel gene which is expressed in kidney and is a candidate for Dent's disease (an X- linked hereditary nephrolithiasis)." Hum Mol Genet **3**(11): 2053-9.

Friedrich, T., T. Breiderhoff and T. J. Jentsch (1999). "Mutational analysis demonstrates that ClC-4 and ClC-5 directly mediate plasma membrane currents." J Biol Chem **274**(2): 896-902.

Fu, D., A. Libson, L. J. Miercke, C. Weitzman, P. Nollert, J. Krucinski and R. M. Stroud (2000). "Structure of a glycerol-conducting channel and the basis for its selectivity." Science **290**(5491): 481-6.

Garman, E. (1999). "Cool data: quantity AND quality." Acta Crystallogr D Biol Crystallogr **55**(Pt 10): 1641-53.

Garman, E. F. and T. R. Schneider (1997). "Macromolecular Cryocrystallography." J. Appl. Cryst. **30**: 211-237.

Gill, S. C. and P. H. von Hippel (1989). "Calculation of protein extinction coefficients from amino acid sequence data." Anal Biochem **182**(2): 319-26.

Grunder, S., A. Thiemann, M. Pusch and T. J. Jentsch (1992). "Regions involved in the opening of CIC-2 chloride channel by voltage and cell volume." Nature **360**(6406): 759-62.

Gunther, W., A. Luchow, F. Cluzeaud, A. Vandewalle and T. J. Jentsch (1998). "ClC-5, the chloride channel mutated in Dent's disease, colocalizes with the proton pump in endocytotically active kidney cells." Proc Natl Acad Sci U S A **95**(14): 8075-80.

Hale, R. S. and G. Thompson (1998). "Codon optimization of the gene encoding a domain from human type 1 neurofibromin protein results in a threefold improvement in expression level in Escherichia coli." Protein Expr Purif **12**(2): 185-8.

Hanahan, D., J. Jessee and F. R. Bloom (1991). "Plasmid transformation of Escherichia coli and other bacteria." Methods Enzymol **204**: 63-113.

Hanke, W. and C. Miller (1983). "Single chloride channels from Torpedo electroplax. Activation by protons." J Gen Physiol **82**(1): 25-45.

Harker, D. (1959). "The determination of the phases of the structure factors of non-centrosymmetric crystals by the method of double isomorphous replacement." Acta Crystallogr **9**(Pt 1): 1-9.

Hendrickson, W. A. (1991). "Determination of macromolecular structures from anomalous diffraction of synchrotron radiation." Science **254**(5028): 51-8.

Ho, Y. S., L. M. Burden and J. H. Hurley (2000). "Structure of the GAF domain, a ubiquitous signaling motif and a new class of cyclic GMP receptor." Embo J **19**(20): 5288-99.

Hoover, D. M., K. R. Rajashankar, R. Blumenthal, A. Puri, J. J. Oppenheim, O. Chertov and J. Lubkowski (2000). "The structure of human beta-defensin-2 shows evidence of higher order oligomerization." J Biol Chem **275**(42): 32911-8.

Jentsch, T. J., T. Friedrich, A. Schriever and H. Yamada (1999). "The CLC chloride channel family." Pflugers Arch **437**(6): 783-95.

Jentsch, T. J. and W. Gunther (1997). "Chloride channels: an emerging molecular picture." Bioessays **19**(2): 117-26.

Jentsch, T. J., C. Lorenz, M. Pusch and K. Steinmeyer (1995). "Myotonias due to CLC-1 chloride channel mutations." Soc Gen Physiol Ser **50**: 149-59.

Jentsch, T. J., K. Steinmeyer and G. Schwarz (1990). "Primary structure of Torpedo marmorata chloride channel isolated by expression cloning in Xenopus oocytes." Nature **348**(6301): 510-4.

Jordt, S. E. and T. J. Jentsch (1997). "Molecular dissection of gating in the ClC-2 chloride channel." Embo J **16**(7): 1582-92.

Jovov, B., Ismailov, II, B. K. Berdiev, C. M. Fuller, E. J. Sorscher, J. R. Dedman, M. A. Kaetzel and D. J. Benos (1995). "Interaction between cystic fibrosis transmembrane conductance regulator and outwardly rectified chloride channels." J Biol Chem **270**(49): 29194-200.

Koch, M. C., K. Steinmeyer, C. Lorenz, K. Ricker, F. Wolf, M. Otto, B. Zoll, F. Lehmann-Horn, K. H. Grzeschik and T. J. Jentsch (1992). "The skeletal muscle chloride channel in dominant and recessive human myotonia." Science **257**(5071): 797-800.

Kornak, U., D. Kasper, M. R. Bosl, E. Kaiser, M. Schweizer, A. Schulz, W. Friedrich, G. Delling and T. J. Jentsch (2001). "Loss of the ClC-7 chloride channel leads to osteopetrosis in mice and man." Cell **104**(2): 205-15.

Kubisch, C., T. Schmidt-Rose, B. Fontaine, A. H. Bretag and T. J. Jentsch (1998). "ClC-1 chloride channel mutations in myotonia congenita: variable penetrance of mutations shifting the voltage dependence." Hum Mol Genet **7**(11): 1753-60.

Kurz, L., S. Wagner, A. L. George, Jr. and R. Rudel (1997). "Probing the major skeletal muscle chloride channel with Zn2+ and other sulfhydryl-reactive compounds." Pflugers Arch **433**(3): 357-63.

Kurz, L. L., H. Klink, I. Jakob, M. Kuchenbecker, S. Benz, F. Lehmann-Horn and R. Rudel (1999). "Identification of three cysteines as targets for the Zn2+ blockade of the human skeletal muscle chloride channel." J Biol Chem **274**(17): 11687-92.

Laemmli, U. K. (1970). "Cleavage of structural proteins during the assembly of the head of bacteriophage T4." Nature **227**(259): 680-5.

Landau, E. M. and J. P. Rosenbusch (1996). "Lipidic cubic phases: a novel concept for the crystallization of membrane proteins." Proc Natl Acad Sci U S A **93**(25): 14532-5.

Larsson, H. P., O. S. Baker, D. S. Dhillon and E. Y. Isacoff (1996). "Transmembrane movement of the shaker K+ channel S4." Neuron **16**(2): 387-97.

Lloyd, L. F., O. S. Gallay, J. Akins and J. G. Zeikus (1994). "Crystallization and preliminary X-ray diffraction studies of xylose isomerase from Thermoanaerobacterium thermosulfurigenes strain 4B." J Mol Biol **240**(5): 504-6.

Lorenz, C., M. Pusch and T. J. Jentsch (1996). "Heteromultimeric CLC chloride channels with novel properties." Proc Natl Acad Sci U S A **93**(23): 13362-6.

Ludewig, U., M. Pusch and T. J. Jentsch (1996). "Two physically distinct pores in the dimeric ClC-0 chloride channel." Nature **383**(6598): 340-3.

Luyckx, V. A., B. Leclercq, L. K. Dowland and A. S. Yu (1999). "Diet-dependent hypercalciuria in transgenic mice with reduced CLC5 chloride channel expression." Proc Natl Acad Sci U S A **96**(21): 12174-9.

MacKinnon, R. (1995). "Pore loops: an emerging theme in ion channel structure." Neuron **14**(5): 889-92.

MacKinnon, R. and D. A. Doyle (1997). "Prokaryotes offer hope for potassium channel structural studies." Nat Struct Biol **4**(11): 877-9.

Maduke, M., C. Miller and J. A. Mindell (2000). "A decade of CLC chloride channels: structure, mechanism, and many unsettled questions." Annu Rev Biophys Biomol Struct **29**: 411-38.

Maduke, M., D. J. Pheasant and C. Miller (1999). "High-level expression, functional reconstitution, and quaternary structure of a prokaryotic ClC-type chloride channel." J Gen Physiol **114**(5): 713-22.

Maduke, M., C. Williams and C. Miller (1998). "Formation of CLC-0 chloride channels from separated transmembrane and cytoplasmic domains." Biochemistry **37**(5): 1315-21.

Matsumura, Y., S. Uchida, Y. Kondo, H. Miyazaki, S. B. Ko, A. Hayama, T. Morimoto, W. Liu, M. Arisawa, S. Sasaki and F. Marumo (1999). "Overt nephrogenic diabetes insipidus in mice lacking the CLC-K1 chloride channel." Nat Genet **21**(1): 95-8.

Matthews, B. W. (1968). "Solvent content of protein crystals." J Mol Biol **33**(2): 491-7.

Middleton, R. E., D. J. Pheasant and C. Miller (1994). "Purification, reconstitution, and subunit composition of a voltage- gated chloride channel from Torpedo electroplax." Biochemistry **33**(45): 13189-98.

Middleton, R. E., D. J. Pheasant and C. Miller (1996). "Homodimeric architecture of a ClC-type chloride ion channel." Nature **383**(6598): 337-40.

Miller, C. and M. M. White (1984). "Dimeric structure of single chloride channels from Torpedo electroplax." Proc Natl Acad Sci U S A **81**(9): 2772-5.

Mindell, J. A., M. Maduke, C. Miller and N. Grigorieff (2001). "Projection structure of a ClC-type chloride channel at 6.5 A resolution." Nature **409**(6817): 219-23.

Miroux, B. and J. E. Walker (1996). "Over-production of proteins in Escherichia coli: mutant hosts that allow synthesis of some membrane proteins and globular proteins at high levels." J Mol Biol **260**(3): 289-98.

Mueller, P. and D. O. Rudin (1963). "Induced excitability in reconstituted cell membrane structure." J Theor Biol **4**(3): 268-80.

Murray, C. B., M. M. Morales, T. R. Flotte, S. A. McGrath-Morrow, W. B. Guggino and P. L. Zeitlin (1995). "CIC-2: a developmentally dependent chloride channel expressed in the fetal lung and downregulated after birth." Am J Respir Cell Mol Biol **12**(6): 597-604.

Nicholas, K. B., Nicholas H.B. Jr., and Deerfield, D.W. II. (1997). GeneDoc: Analysis and Visualization of Genetic Variation. BioInformer. **4**.

Nobile, M., M. Pusch, C. Rapisarda and S. Ferroni (2000). "Single-channel analysis of a ClC-2-like chloride conductance in cultured rat cortical astrocytes." FEBS Lett **479**(1-2): 10-4.

Oliver, D., D. Z. He, N. Klocker, J. Ludwig, U. Schulte, S. Waldegger, J. P. Ruppersberg, P. Dallos and B. Fakler (2001). "Intracellular anions as the voltage sensor of prestin, the outer hair cell motor protein." Science **292**(5525): 2340-3.

Ostermeier, C. and H. Michel (1997). "Crystallization of membrane proteins." Curr Opin Struct Biol **7**(5): 697-701.

Palczewski, K., T. Kumasaka, T. Hori, C. A. Behnke, H. Motoshima, B. A. Fox, I. Le Trong, D. C. Teller, T. Okada, R. E. Stenkamp, M. Yamamoto and M. Miyano (2000). "Crystal structure of rhodopsin: A G protein-coupled receptor." Science **289**(5480): 739-45.

Papazian, D. M., L. C. Timpe, Y. N. Jan and L. Y. Jan (1991). "Alteration of voltage-dependence of Shaker potassium channel by mutations in the S4 sequence." Nature **349**(6307): 305-10.

Papiz, M. Z., A. M. Hawthornthwaite, R. J. Cogdell, K. J. Woolley, P. A. Wightman, L. A. Ferguson and J. G. Lindsay (1989). "Crystallization and characterization of two crystal forms of the B800- 850 light-harvesting complex from Rhodopseudomonas acidophila strain 10050." J Mol Biol **209**(4): 833-5.

Piwon, N., W. Gunther, M. Schwake, M. R. Bosl and T. J. Jentsch (2000). "CIC-5 Cl--channel disruption impairs endocytosis in a mouse model for Dent's disease." Nature **408**(6810): 369-73.

Pusch, M. (1996). "Knocking on channel's door. The permeating chloride ion acts as the gating charge in ClC-0." J Gen Physiol **108**(4): 233-6.

Pusch, M., U. Ludewig, A. Rehfeldt and T. J. Jentsch (1995a). "Gating of the voltage-dependent chloride channel CIC-0 by the permeant anion." Nature **373**(6514): 527-31.

Pusch, M., K. Steinmeyer, M. C. Koch and T. J. Jentsch (1995b). "Mutations in dominant human myotonia congenita drastically alter the voltage dependence of the CIC-1 chloride channel." Neuron **15**(6): 1455-63.

Rosenbohm, A., R. Rudel and C. Fahlke (1999). "Regulation of the human skeletal muscle chloride channel hClC-1 by protein kinase C." J Physiol **514**(Pt 3): 677-85.

Rost, B. and C. Sander (1993). "Prediction of protein secondary structure at better than 70% accuracy." J Mol Biol **232**(2): 584-99.

Sansom, M. S. and H. Weinstein (2000). "Hinges, swivels and switches: the role of prolines in signalling via transmembrane alpha-helices." Trends Pharmacol Sci **21**(11): 445-51.

Saviane, C., F. Conti and M. Pusch (1999). "The muscle chloride channel ClC-1 has a double-barreled appearance that is differentially affected in dominant and recessive myotonia." J Gen Physiol **113**(3): 457-68.

Schmidt-Rose, T. and T. J. Jentsch (1997). "Reconstitution of functional voltage-gated chloride channels from complementary fragments of CLC-1." J Biol Chem **272**(33): 20515-21.

Schmidt-Rose, T. and T. J. Jentsch (1997). "Transmembrane topology of a CLC chloride channel." Proc Natl Acad Sci U S A **94**(14): 7633-8.

Schwappach, B., S. Stobrawa, M. Hechenberger, K. Steinmeyer and T. J. Jentsch (1998). "Golgi localization and functionally important domains in the NH2 and COOH terminus of the yeast CLC putative chloride channel Gef1p." J Biol Chem **273**(24): 15110-8.

Shen, M. R., S. N. Wu and C. Y. Chou (1996). "Volume-sensitive chloride channels in the primary culture cells of human cervical carcinoma." Biochim Biophys Acta **1315**(2): 138-44.

Sigworth, F. J. (1994). "Voltage gating of ion channels." Q Rev Biophys **27**(1): 1-40.

Simon, D. B., R. S. Bindra, T. A. Mansfield, C. Nelson-Williams, E. Mendonca, R. Stone, S. Schurman, A. Nayir, H. Alpay, A. Bakkaloglu, J. Rodriguez-Soriano, J. M. Morales, S. A. Sanjad, C. M. Taylor, D. Pilz, A. Brem, H. Trachtman, W. Griswold, G. A. Richard, E. John and R. P. Lifton (1997). "Mutations in the chloride channel gene, CLCNKB, cause Bartter's syndrome type III." Nat Genet **17**(2): 171-8.

Smith, R. L., G. H. Clayton, C. L. Wilcox, K. W. Escudero and K. J. Staley (1995). "Differential expression of an inwardly rectifying chloride conductance in rat brain neurons: a potential mechanism for cell-specific modulation of postsynaptic inhibition." J Neurosci **15**(5 Pt 2): 4057-67.

Soroceanu, L., T. J. Manning, Jr. and H. Sontheimer (1999). "Modulation of glioma cell migration and invasion using Cl(-) and K(+) ion channel blockers." J Neurosci **19**(14): 5942-54.

Steinmeyer, K., R. Klocke, C. Ortland, M. Gronemeier, H. Jockusch, S. Grunder and T. J. Jentsch (1991a). "Inactivation of muscle chloride channel by transposon insertion in myotonic mice." Nature **354**(6351): 304-8.

Steinmeyer, K., C. Ortland and T. J. Jentsch (1991b). "Primary structure and functional expression of a developmentally regulated skeletal muscle chloride channel." Nature **354**(6351): 301-4.

Stobrawa, S. M., T. Breiderhoff, S. Takamori, D. Engel, M. Schweizer, A. A. Zdebik, M. R. Bosl, K. Ruether, H. Jahn, A. Draguhn, R. Jahn and T. J. Jentsch (2001). "Disruption of ClC-3, a chloride channel expressed on synaptic vesicles, leads to a loss of the hippocampus." Neuron **29**(1): 185-96.

Stroffekova, K., E. Y. Kupert, D. H. Malinowska and J. Cuppoletti (1998). "Identification of the pH sensor and activation by chemical modification of the ClC-2G Cl- channel." Am J Physiol **275**(4 Pt 1): C1113-23.

Studier, F. W. and B. A. Moffatt (1986). "Use of bacteriophage T7 RNA polymerase to direct selective high-level expression of cloned genes." J Mol Biol **189**(1): 113-30.

Stuhmer, W., F. Conti, H. Suzuki, X. D. Wang, M. Noda, N. Yahagi, H. Kubo and S. Numa (1989). "Structural parts involved in activation and inactivation of the sodium channel." Nature **339**(6226): 597-603.

Thiemann, A., S. Grunder, M. Pusch and T. J. Jentsch (1992). "A chloride channel widely expressed in epithelial and non-epithelial cells." Nature **356**(6364): 57-60.

Thompson, J. D., D. G. Higgins and T. J. Gibson (1994). "CLUSTAL W: improving the sensitivity of progressive multiple sequence alignment through sequence weighting, position-specific gap penalties and weight matrix choice." Nucleic Acids Res **22**(22): 4673-80.

Tieleman, D. P., I. H. Shrivastava, M. R. Ulmschneider and M. S. Sansom (2001). "Proline-induced hinges in transmembrane helices: Possible roles in ion channel gating." Proteins **44**(2): 63-72.

Timmins, P. A., J. Hauk, T. Wacker and W. Welte (1991). "The influence of heptane-1,2,3-triol on the size and shape of LDAO micelles. Implications for the crystallisation of membrane proteins." FEBS Lett **280**(1): 115-20.

Titchmarsh, E. C. (1937). Introduction to the Theory of Fourier Integrals. Oxford, Clarendon Press.

Ullrich, N., A. Bordey, G. Y. Gillespie and H. Sontheimer (1998). "Expression of voltage-activated chloride currents in acute slices of human gliomas." Neuroscience **83**(4): 1161-73.

Ullrich, N., G. Y. Gillespie and H. Sontheimer (1996). "Human astrocytoma cells express a unique chloride current." Neuroreport **7**(5): 1020-4.

Vaananen, H. K., H. Zhao, M. Mulari and J. M. Halleen (2000). "The cell biology of osteoclast function." J Cell Sci **113**(Pt 3): 377-81.

Valverde, M. A. (1999). "CIC channels: leaving the dark ages on the verge of a new millennium." Curr Opin Cell Biol **11**(4): 509-16.

Waldegger, S. and T. J. Jentsch (2000). "From tonus to tonicity: physiology of CLC chloride channels." J Am Soc Nephrol **11**(7): 1331-9.

Wollnik, B., C. Kubisch, K. Steinmeyer and M. Pusch (1997). "Identification of functionally important regions of the muscular chloride channel CIC-1 by analysis of recessive and dominant myotonic mutations." Hum Mol Genet **6**(5): 805-11.

Xiong, H., C. Li, E. Garami, Y. Wang, M. Ramjeesingh, K. Galley and C. E. Bear (1999). "ClC-2 activation modulates regulatory volume decrease." J Membr Biol **167**(3): 215-21.

Yang, N., A. L. George, Jr. and R. Horn (1996). "Molecular basis of charge movement in voltage-gated sodium channels." Neuron **16**(1): 113-22.